Direct Measurement of Metal Concentrations in Fluid Inclusions, a Tale of Hydrothermal Alteration and REE Ore Formation from Strange Lake, Canada

O.V. Vasyukova and A.E. Williams-Jones

Department of Earth and Planetary Sciences, McGill University, 3450 University Street, Montreal, Québec, Canada, H3A 0E8, olga.vasyukova@mcgill.ca

Abstract

Granites and pegmatites in the Strange Lake pluton experienced extreme enrichment in high field strength elements (HFSE), including the rare earth elements (REE). Much of this enrichment took place in the most altered rocks, and is expressed as secondary minerals, showing that hydrothermal fluids played an important role in HFSE concentration. Vasyukova et al. (2016) reconstructed a P-T-X path for the evolution of these fluids and provided evidence that hydrothermal activity was initiated by exsolution of fluid during crystallisation of border zone pegmatites (at ~450-500 ^{o}C and 1.1 kbar). This early fluid comprised a high salinity (25 wt.% NaCl) aqueous phase and a CH_4+H_2 gas. During cooling, the gas was gradually oxidised, first to higher hydrocarbons (e.g., C_2H_6, C_3H_8), and then to CO_2, and the salinity decreased to 4 wt.% (~250-300 ^{o}C), before increasing to 19 wt.%, due to fluid-rock interaction (~150 ^{o}C). Here we present crush-leach fluid inclusion data on the concentrations of the REE and major ligands at different stages of the evolution of the fluid.

The chondrite-normalised REE profile of the fluid evolved from light REE (La-Nd)-enriched at high temperature (~400 ^{o}C, Stages 1-2a) to middle REE (Sm-Er)-enriched at 360 to 250 ^{o}C (Stages 2b-3) and strongly heavy REE (Tm-Lu)-enriched at low temperature (150 ^{o}C, Stage 5). These changes in the REE distribution were accompanied by changes in the concentrations of major ligands, i.e., Cl^- was the dominant ligand in Stages 1, 2, 4 and 5, whereas HCO_3^- was dominant in Stage 3. The fluorine content decreased from 0.6 wt.% in Stage 2a to 0.1-0.4 wt.% in Stages 2b and 3 and to 0.05 wt.% in Stages 4-5.

Alteration of arfvedsonite to aegirine and/or hematite contributed strongly to the mobilisation of the REE. This alteration released middle REE (MREE) and heavy REE (HREE), which either partitioned into the fluid or precipitated directly as bastnäsite-(Ce), ferri-allanite-(Ce) or

Vasyukova, O. V. and A. E. Williams-Jones. "Direct Measurement of Metal Concentrations in Fluid Inclusions, a Tale of Hydrothermal Alteration and Ree Ore Formation from Strange Lake, Canada."
Chemical Geology 483 (Apr 20 2018): 385-96. http://dx.doi.org/10.1016/j.chemgeo.2018.03.003.

gadolinite-(Y). Replacement of primary fluorbritholite-(Ce) that crystallised from an immiscible fluoride melt, which altered to bastnäsite-(Ce), was also important in mobilising the REE (MREE). This is shown by the fact that the REE content of the bastnäsite-(Ce) is less than half of that of the fluorbritholite-(Ce).

This paper presents the first report of the distribution of the REE in an evolving hydrothermal fluid. Using this distribution, in conjunction with information on the changing physicochemical conditions, the study identifies the sources of REE enrichment, reconstructs the path of REE concentration, and evaluates the REE mineralising capacity of the fluid. Finally, this information is integrated into a predictive model for REE mobilisation applicable not only to Strange Lake but any REE ore-forming system, in which hydrothermal processes were important.

Introduction

Fluid inclusions have been intensively studied for almost half a century and used to characterise the major properties of natural fluids, especially those involved in metallic mineral ore formation (Roedder, 1977; Roedder, 1984; Craig and Vaughan, 1994; Wilkinson, 2001). Indeed, many and perhaps a preponderance of papers dealing with the genesis of hydrothermal ore deposits contain a section reporting results of microthermometric measurements of fluid inclusions that are used to make inferences about the physicochemical conditions of mineralisation. These measurements have provided important information on the pressure-temperature conditions and the concentrations of the major cations and ligands in the fluid (Roedder, 1984; Roedder, 1997). In turn, they have been used to infer mechanisms of ore mineral deposition, such as boiling (or effervescence, i.e., exsolution of a gas like CO_2), fluid-rock interaction and fluid mixing (Skinner and Barton, 1973; Skinner, 1979; Wilkinson, 2001; Heinrich, 2007). Information on the concentrations of the ore metals and other trace elements, however, had to await the development of micro-analytical techniques, notably Laser Ablation Inductively Coupled Plasma Mass Spectrometry (LA-ICP-MS) of individual fluid inclusions (Shepherd and Chenery, 1995; Audetat et al., 1998; Longerich, 2008; Pettke, 2008) and Inductively Coupled Plasma Mass Spectrometry (ICP-MS) or Inductively Coupled Plasma Atomic Emission Spectrometry (ICP-AES) of extracted fluids (Bottrell et al., 1988; Banks and Yardley, 1992; Ghazi et al., 1993; Banks et al., 1994).

Here, we report results of the application of ICP-MS to fluids extracted from fluid inclusions using the crush-leach method, in which a small sample of the mineral hosting the fluid inclusions (quartz) is crushed and the fluid released into a matrix or leach solution that is subsequently

Vasyukova, O. V. and A. E. Williams-Jones. "Direct Measurement of Metal Concentrations in Fluid Inclusions, a Tale of Hydrothermal Alteration and Ree Ore Formation from Strange Lake, Canada." Chemical Geology 483 (Apr 20 2018): 385-96. http://dx.doi.org/10.1016/j.chemgeo.2018.03.003.

analysed for its trace element content by ICP-MS. Ion Chromatography (IC) complements analyses of the extracted fluid by providing a rare opportunity to analyse anionic species such as fluoride (F^-), chloride (Cl^-), bromide (Br^-), nitrate (NO_3^-), phosphate (PO_4^{3-}) and sulphate (SO_4^{2-}), something that is not possible using methods applicable to the analysis of individual inclusions. Another advantage of the crush-leach method is that it can be used to analyse elements, such as the REE and other HFSE, which are typically present in hydrothermal fluids in concentrations below those that can be detected in single inclusions using LA-ICP-MS. There are two important limitations to the application of the crush leach method. Firstly, the quartz grains separated for analysis must be of high purity and not contain crystals of other minerals (attached to the surface or as inclusions) and secondly the fluid inclusions should be dominated by inclusions of a single population, which is generally not the case. Nonetheless, provided great care is taken to avoid contamination during sample preparation, especially during sample crushing (e.g., by using a clean room), it is possible to obtain high quality data for some ore-forming systems.

Despite the obvious advantages of the crush-leach method, and the fact that it provides the only means for reliably analysing the REE and other HFSE, there have been relatively few applications of this method. In the case of the REE, the studies have been restricted to Norman et al. (1989), Ghazi et al. (1993), Banks et al. (1994), Bühn and Rankin (1999) and Bühn et al. (2002). Of these studies, however, only that of Banks et al. (1994) dealt with REE mineralisation. This is particularly surprising given the sharp increase in the number of studies that have been devoted to hydrothermal REE deposits during the past five years.

In this paper, we report the results of crush-leach experiments applied to samples from pegmatites, which host the potentially economic REE mineralisation of the Strange Lake pluton (Gysi and Williams-Jones, 2013). Building on a previous study of the physicochemical evolution of fluids in granites and pegmatites of Strange Lake (Vasyukova et al., 2016), we present the first comprehensive analyis of REE fluid chemistry in an evolving REE ore-forming hydrothermal system. In so doing, we evaluate the REE and related ligand concentrations at different stages in the evolution of the fluids in the context of their mineralising capacity, identify the sources of REE enrichment of the fluid and develop a predictive model for REE mobilisation in the system.

Vasyukova, O. V. and A. E. Williams-Jones. "Direct Measurement of Metal Concentrations in Fluid Inclusions, a Tale of Hydrothermal Alteration and Ree Ore Formation from Strange Lake, Canada."
Chemical Geology 483 (Apr 20 2018): 385-96. http://dx.doi.org/10.1016/j.chemgeo.2018.03.003.

Geological setting

The Mid-Proterozoic (1240 ± 2 Ma; (Miller et al., 1997) Strange Lake pluton comprises three main intrusive phases, namely hypersolvus granite, transsolvus granite and pegmatite (Fig. 1), with the granitic phases being distinguished mainly on the basis of feldspar mineralogy (Nassif, 1993) and arfvedsonite morphology (Siegel et al., 2017). The earliest and the least evolved phase is the hypersolvus granite, which occupies the central part of the intrusion, and is characterised by the presence of perthite as the only feldspar and interstitial arfvedsonite. Perthite is also present in the transsolvus granite, which is more evolved, volumetrically much more abundant, and occupies the outer part of the pluton. In addition, however, the transsolvus granite contains primary microcline and albite, and the arfvedsonite, instead of being an interstitial phase, occurs as phenocrysts.

The pegmatites occur near the top of the pluton as sub-horizontal sheets and lenses ranging from a few cm to 10 m in thickness. They are concentrated in two fields, one adjacent to its northwest margin, the B-Zone, and the other near its geographic centre, the Main-Zone (Fig. 1). These fields host REE-Zr-Nb mineralisation that has been considered for economic exploitation. Indeed, recent exploration of the B-Zone has identified an indicated resource of 278 Mt of ore, grading 0.94 wt. % REE_2O_3 (38% heavy rare-earth oxides), 1.92 wt. % ZrO_2 and 0.18 wt. % Nb_2O_5. This includes a high grade spine containing 20 Mt of ore grading 1.44 wt.% REE_2O_3 (50% heavy rare-earth oxides), 2.59 wt. % ZrO_2 and 0.34 wt. % Nb_2O_5 (www.questrareminerals.com). Many of the pegmatites are mineralogically zoned from a border containing coarse-grained euhedral alkali feldspar, quartz, arfvedsonite and titano- and zircono-silicate minerals to a core dominated by quartz and fluorite with variable proportions of REE minerals. The contacts between the pegmatites and granite vary from diffuse to sharp, and locally an aplite layer marks the contact.

Evidence of hydrothermal alteration is widespread in the transsolvus granite and increases in intensity towards the pegmatite fields. Perthite and K-feldspar in the transsolvus granite were albitised, as was K-feldspar in the pegmatites, whereas albite in the latter was transformed to microcline. Arfvedsonite in both units was altered to aegirine and/or hematite. Calcium metasomatism was pervasive in the pegmatites and locally pervasive in the adjacent transsolvus granite, leading to the replacement of sodium titanosilicates and zirconosilicates by calcium minerals such as titanite and gittinsite ($CaSi_2O_7$), respectively. Finally, late phyllic alteration, manifested by the replacement of primary and secondary feldspars with Al- and Fe-rich

Vasyukova, O. V. and A. E. Williams-Jones. "Direct Measurement of Metal Concentrations in Fluid Inclusions, a Tale of Hydrothermal Alteration and Ree Ore Formation from Strange Lake, Canada." Chemical Geology 483 (Apr 20 2018): 385-96. http://dx.doi.org/10.1016/j.chemgeo.2018.03.003.

phyllosilicates, was also pervasive and developed locally in the adjacent transsolvus granite (Gysi and Williams-Jones, 2013; Gysi et al., 2016).

Previous work

In an earlier publication (Vasyukova et al., 2016), we characterised the fluid trapped in inclusions in quartz from the Strange Lake granites and pegmatites, and interpreted the evolution of this fluid based on fluid inclusion microthermometry, bulk gas analyses and thermodynamic calculations. This evolution is illustrated in summary form in Figure 2 and reflects a system in which the pegmatites "stewed in their own juices".

A fluid containing immiscible aqueous (25 wt.% NaCl eq.) and gas-rich carbonic (CH_4 + up to 20 mol.% H_2) phases (Group 1 in Fig. 2) exsolved from a magma at ~450-500 °C and an oxygen fugacity 7.3 units below the quartz-fayalite-magnetite (QFM) buffer. Cooling to ~ 425 °C induced oxidation, which resulted in an increase in fO_2 to ~ 6.2 log units below the QFM buffer, causing the fluid to become CH_4-dominant; the proportion of H_2 decreased to ~3 mol.% (Group 2a in Fig. 2). The evolution described above is recorded by Group 1 and 2a inclusions and constitutes Stage 1-2a of the fluid evolution, which is characterised by an absence of hydrothermal alteration.

Stage 2b-3 commenced at ~325-360 °C when further oxidation (~2.8 log units below the QFM buffer) triggered alteration of arfvedsonite to aegirine. The alteration buffered fO_2 and prevented formation of CO_2 from CH_4; instead, it facilitated oxidative coupling of methane, which produced higher order hydrocarbons (e.g., C_2H_6 and C_3H_8). As a result of the fluid-rock interaction, the salinity of the fluid decreased progressively from ~25 to ~14 wt.% NaCl eq. (Group 2b in Fig. 2) and eventually, alteration ceased because the fluid salinity was insufficient for the reaction (see Vasyukova et al., 2016; Reaction 3) to proceed further. During subsequent cooling to ~300 ^{o}C, the system was unbuffered and oxygen fugacity consequently increased to 1.2 log units below the QFM buffer causing the fluid to become CO_2-dominated (Group 3 in Fig. 2). The newly formed CO_2 reacted with H_2O in the fluid to produce HCO_3^-, which, in turn, reacted with the Na^+ ions, precipitating nahcolite. This, together with further dilution, due to fluid-rock interaction, lead to an additional decrease in salinity from ~14 to ~4 wt.% NaCl eq. (late Group 3 in Fig. 2). The production of HCO_3^- was accompanied by production of H^+, which sharply lowered the pH of the fluid, causing it to attack Na-rich minerals, such as elpidite,

Vasyukova, O. V. and A. E. Williams-Jones. "Direct Measurement of Metal Concentrations in Fluid Inclusions, a Tale of Hydrothermal Alteration and Ree Ore Formation from Strange Lake, Canada." Chemical Geology 483 (Apr 20 2018): 385-96. http://dx.doi.org/10.1016/j.chemgeo.2018.03.003.

narsarsukite and arfvedsonite. Elpidite and narsarsukite were replaced, leaving behind pseudomorphs filled by quartz, hematite and gittinsite or titanite, respectively; the arfvedsonite was replaced by aegirine and/or hematite.

Stage 4-5 began when the carbonic component was removed at ~225 °C due to fluid-rock interaction and migration of CO_2 out of the pegmatites. Oxidation continued (2.8 log units above the QFM buffer at 225 °C) as did fluid-rock interaction (intense hematisation and formation of phyllosilicates), which caused an increase in salinity to almost the initial level, ~19 wt.% NaCl eq. at ~150°C (Group 5 in Fig. 2).

Samples

Samples for this study (see Fig. 1 for locations) were chosen in such a way as to represent the different stages in the evolution of the fluid. Stage 1-2a is represented by Sample 16, which is from the border zone of an unaltered pegmatite, and is dominated by Group 2a fluid inclusions (Figs. 2, 3a). This stage was followed by Stage 2b, which is represented by Sample 13 (Fig. 3b) from the massive quartz core of a weakly altered pegmatite (arfvedsonite crystals were altered to aegirine along their rims), and only contains Group 2b fluid inclusions.

Sample 11, representing Stage 3, consists of massive quartz from the core of a strongly altered pegmatite, in which arfvedsonite was pervasively altered to aegirine (±hematite), and pseudomorphs after elpidite and narsarsukite are common (Fig. 3c). The sample mainly contains Group 3 fluid inclusions, although a small proportion of earlier Group 2 fluid inclusions are observed. Sample 2 also contains Group 3 fluid inclusions, but represents late Stage 3. This sample is from a quartz vein that crosscut the host hypersolvus granite (Fig. 3d). Within the adjacent granite, arfvedsonite was altered to aegirine. Four zones were observed from the vein outwards: 1) aegirine with no arfvedsonite remnants (identified as ‘Aeg(E)’ in Fig. 3d); 2) aegirine with fluorite and rare arfvedsonite remnants (identified as ‘Aeg(E)+Fl’ in Fig. 3d); 3) aegirine with arfvedsonite remnants (identified as ‘Aeg(E)+Arf’ in Fig. 3d); and 4) weakly altered arfvedsonite (marked as ‘Arf’ in Fig. 3d).

Sample 7 represents Stages 4 and 5, and is from the core of a strongly altered pegmatite, in which pervasive hematisation was observed; even within the massive quartz of the core, hematite precipitated along fractures (Fig. 3e). The sample is dominated by roughly equal proportions of

Vasyukova, O. V. and A. E. Williams-Jones. "Direct Measurement of Metal Concentrations in Fluid Inclusions,
a Tale of Hydrothermal Alteration and Ree Ore Formation from Strange Lake, Canada."
Chemical Geology 483 (Apr 20 2018): 385-96. http://dx.doi.org/10.1016/j.chemgeo.2018.03.003.

two groups of fluid inclusions, namely Groups 4 and 5. Group 4 inclusions are primary and aqueous (liquid-vapour) and Group 5 inclusions are secondary and also aqueous (liquid-vapour). Although a single inclusion population is usually a prerequisite for bulk analyses, we included Sample 7 in our study because this sample is the only one that represents hematisation. Even if we could not distinguish between Group 4 and 5 fluids, a mixture of these fluids provides important information about Stages 4 and 5.

Three samples (see Fig. 1 for locations) were chosen to characterise the fluid responsible for the alteration of arfvedsonite to aegirine or to hematite and aegirine. Sample 204705 contains pegmatite-sized (up to 5 cm) crystals of arfvedsonite with rims replaced by aegirine and cores partly replaced by hematite. Sample BZ10076-11 contains crystals displaying the same type of alteration but at a more advanced stage, i.e., there is no visible arfvedsonite, only aegirine rims and hematite cores. Sample 2, mentioned above, contains late aegirine that precipitated along fractures in a quartz vein (identified as 'Aeg(L)' in Fig. 3d).

Methodology

Bulk fluid analysis

Crush-leach

The crush-leach procedure employed in this study is a slightly modified version of the procedure described by Banks et al. (1994). Quartz grains (on average 1.5-2 g per sample) were hand-picked under a binocular microscope making sure that they do not contain crystals of minerals other than quartz. The grains were then cleaned. This involved three cycles of repeated rinsing of the samples in nanopure water (15-20 rinses) followed by soaking in hot (~70 ^{o}C) concentrated nitric acid for 1.5-2 hours. The samples were dried after each cycle in a drying oven at ~60 °C overnight.

To suppress adsorption of polyvalent cations on fresh quartz surfaces, we spiked the leaching solution (3 wt.% HNO_3) with uranium (200 ppm). Uranium was chosen as the spike because of its high valence and high solubility in oxidised aqueous solutions at room temperature. This makes it a particularly strong candidate to be adsorbed onto the surface of quartz, and to therefore prevent the adsorption of other highly charged elements. A stock uranium solution (1,000 ppm of U in 3 wt.% HNO_3) was purchased from Fisher Scientific (Catalog No. PU1KN-100). Ultra-pure water and Optima$^{@}$ grade 69 wt.% nitric acid were used to prepare the solutions.

Vasyukova, O. V. and A. E. Williams-Jones. "Direct Measurement of Metal Concentrations in Fluid Inclusions, a Tale of Hydrothermal Alteration and Ree Ore Formation from Strange Lake, Canada." Chemical Geology 483 (Apr 20 2018): 385-96. http://dx.doi.org/10.1016/j.chemgeo.2018.03.003.

Each cleaned and dried sample was divided in half to prepare samples for ICP-MS (metals), AA (Ca) and IC (ligands) analyses. The only difference in preparation of the samples for ICP-MS (and AA) and IC analyses is that samples for the former were crushed in uranium-doped 3 wt.% HNO_3 leaching solution, whereas samples for IC were crushed in ultrapure water. This and the subsequent steps in the procedure were conducted in a clean room to prevent contamination. The cleaned samples were crushed in an agate mortar (samples were submerged in the leaching solution), and the leachate solution was extracted, filtered (0.45 µm) and analysed. Blank samples of inclusion-free Brazilian quartz were prepared in exactly the same way, i.e., with uranium-doped 3 wt.% HNO_3 leaching solution for ICP-MS (and AA) and ultrapure water for IC.

Inductively Coupled Plasma Mass Spectrometry

For the purpose of the analyses, a certified multi-element standard (10 ppm; 40 elements in 3 wt.% HNO_3) was purchased from SCP Science (http://www.scpscience.com/). Seven solutions containing different concentrations of this standard solution (500, 100, 20, 5, 1, 0.5 and 0.2 ppb) were prepared and a calibration curve constructed. As with the earlier sample preparation, the standard dilutions were performed in a clean room. The samples, sample blanks, standard solutions and solution blanks were analysed with ICP-MS at the department of Earth and Planetary Sciences, McGill University, with a Thermo Finnigan iCapQ ICP-MS coupled to an auto-sampler for analysis of solutions. The dwell time for analyses was 10 ms and the number of sweeps was set to 100. The following isotopes were analysed: ^{7}Li, ^{23}Na, ^{39}K, ^{45}Sc, ^{57}Fe, ^{66}Zn, ^{89}Y, ^{90}Zr, ^{139}La, ^{140}Ce, ^{141}Pr, ^{142}Nd, ^{146}Nd, ^{147}Sm, ^{153}Eu, ^{155}Gd, ^{157}Gd, ^{159}Tb, ^{163}Dy, ^{165}Ho, ^{166}Er, ^{169}Tm, ^{172}Yb, ^{173}Yb, ^{175}Lu. All counts per second were converted to concentrations in ppb using the calibration curve referred to above. Concentrations calculated for each element from the signal for the blank solution were treated as the detection limit.

Atomic Absorption (AA)

Calcium concentrations were measured by Atomic Absorption Spectroscopy (AA) to avoid possible interference of the ICP-MS signal for ^{44}Ca with those for $^{12}C^{16}O_2$, $^{14}N_2{}^{16}O^{+}$and $^{28}Si^{16}O^{+}$. The analyses were performed in the Department of Earth and Planetary Sciences at McGill University with a Perkin Elmer AAnalyst 100 Flame atomic absorption spectrometer. A calibration curve was prepared using six standards with concentrations ranging from 0.3 to 2.6 ppm.

Vasyukova, O. V. and A. E. Williams-Jones. "Direct Measurement of Metal Concentrations in Fluid Inclusions, a Tale of Hydrothermal Alteration and Ree Ore Formation from Strange Lake, Canada."
Chemical Geology 483 (Apr 20 2018): 385-96. http://dx.doi.org/10.1016/j.chemgeo.2018.03.003.

Ion exchange Chromatography (IC)

Ligand concentrations were measured by Dr. Dirk Kirste of the Department of Earth Sciences, Simon Fraser University, using a Dionex ICS-3000 SP Ion Chromatograph equipped with an AS22 column and a 500 µl sample loading loop. Samples were analysed for fluoride (F^-), chloride (Cl^-) and sulphate (SO_4^{2-}) ions. Detection limits were 5 ppb for F^-, 100 ppb for Cl^- and 20 ppb for SO_4^{2-}.

Data treatment (normalisation)

As the concentrations of metals and ligands were determined using separate aliquots of quartz and different leaching solutions, it was necessary to normalise the two sets of leachate data. This was done by analysing the K concentrations of both the leaching solutions, and correcting the ligand concentrations by multiplying their values by the ratio of the K concentration in the metal solution over that in the ligand solution. The corrected data for the analysed solutions are listed in Table 1. The absolute concentrations of the metals in the bulk fluids were calculated by normalising the above data to the apparent average salinity using the Cl concentrations of fluid inclusions determined microthermometrically by Vasyukova et al. (2016). These concentrations are reported in Table 2.

Mineral analysis

The major and trace compositions of arfvedsonite, aegirine and hematite were determined using Electron Microprobe Analysis (EMPA) and Laser Ablation Inductively Coupled Plasma Mass Spectrometry (LA-ICPMS). The former analyses were performed with a JEOL JXA-8900L electron microprobe located at McGill University (Department of Earth and Planetary Sciences), using a beam diameter of 15 µm, a beam current of 20 nA and an acceleration voltage of 20 kV. The standards employed in the analyses, the counting times and the detection limits for the different elements are reported in Table 3.

Laser ablation ICP-MS analyses were carried out on the same spots that had been analysed using the electron microprobe. These analyses were carried out using a NewWave 213 nm Nd-YAG laser-ablation system and a Thermo Finnigan iCapQ ICP-MS in the Department of Earth and Planetary Sciences at McGill University. The analyses involved a 10 Hz repetition rate, and 40 µm beam diameter; the NIST 610 glass was used as an internal standard for Si. Data from the

Vasyukova, O. V. and A. E. Williams-Jones. "Direct Measurement of Metal Concentrations in Fluid Inclusions, a Tale of Hydrothermal Alteration and Ree Ore Formation from Strange Lake, Canada." Chemical Geology 483 (Apr 20 2018): 385-96. http://dx.doi.org/10.1016/j.chemgeo.2018.03.003.

electron microprobe analyses were used to normalise the LA-ICP-MS data. The results of the analyses are reported in Table 4.

Thermodynamic calculations

Thermodynamic calculations were performed to estimate the pH of the fluid in equilibrium with different mineral assemblages at different temperatures, and to model the capacity of the fluid to transport the rare earth elements. For this, we used the software package HCh (Shvarov, 1999; Shvarov and Bastrakov, 1999). The sources of the thermodynamic data for the minerals, gases and aqueous complexes are listed in Table 5.

Results

Pegmatite Core

The composition of the fluid in the pegmatite cores was determined from fluid extracted from Samples 7, 11 and 13. The three samples consist almost entirely of quartz, and contain fluids trapped during Stages 4-5, 3 and 2b, respectively. Their measured rare earth element contents, in each case, were well above the concentrations of the procedural blanks (Table 1).

Sample 7

As was mentioned earlier, Sample 7 contains a mix of aqueous Group 4 and 5 inclusions (Type IV; see Vasyukova et al., 2016 for descriptions of these fluid inclusion types). Consequently, there is a significant range in salinity (Vasyukova et al., 2016). In order to establish a representative salinity, we therefore calculated the median salinity of the Group 4 and 5 fluid inclusion population from the median salinity for the individual fluid inclusion assemblages reported in Appendix A of Vasyukova et al. (2016). This salinity is 10 wt.% NaCl eq., the value to which the composition of the extracted fluid was normalised (Table 2). Based on the results of the crush-leach experiment, Sample 7 contains 6.0 wt.% Cl, 2.75 wt.% Na, 0.5 wt.% Ca, 0.08 wt.% K and 0.05 wt.% F; the sulphate concentration is 0.2 wt.% (Table 2). A calculation of the cation-anion charge balance revealed an excess of anions of 8.8 %, which is a very good result and provides confidence that the analyses are reliable.

Our results show that the Sample 7 fluid has REE concentrations ranging between 0.05 ppm (Eu) and 24 ppm (Yb), and a total REE (including Y and Sc) concentration of 49 ppm. They also show that among the even-numbered lanthanides, Er and Yb have the highest concentrations, i.e.,

Vasyukova, O. V. and A. E. Williams-Jones. "Direct Measurement of Metal Concentrations in Fluid Inclusions, a Tale of Hydrothermal Alteration and Ree Ore Formation from Strange Lake, Canada." Chemical Geology 483 (Apr 20 2018): 385-96. http://dx.doi.org/10.1016/j.chemgeo.2018.03.003.

the fluid is HREE-enriched (Table 2). The yttrium concentration is also high, consistent with the classification of this element as a HREE. This distribution of REE concentrations is clearly evident when the data are normalised to chondrite. The profile is flat for the light REE (LREE), displays a weak positive anomaly for Sm and a strong negative anomaly for Eu, and increases sharply from Ho to Lu (Fig. 4).

Sample 11

The Group 3 inclusions that dominate Sample 11 comprise roughly equal proportions of Type IV (aqueous), V (aqueous-CO_2), VI-1 (aqueous, trapped nahcolite) and VI-2 (aqueous, nahcolite crystallised on freezing) inclusions, each of which contributed to the bulk salinity (see Vasyukova et al., 2016 for more complete definitions of the fluid inclusion types). The median salinity of the Type IV inclusions is 10 wt.% NaCl. eq., whereas that of the Type V and VI (1 and 2) inclusions is 4.2-4.7 and 4.2 wt.% NaCl eq., respectively (Vasyukova et al. 2016). Accordingly, the fluid extracted from Sample 11 was estimated to have a salinity of 6 wt.% NaCl. We therefore normalised the composition of this fluid to the corresponding Cl content (3.6 wt.%). Based on this normalisation, the major element composition of the fluid is 3.7 wt.% Na, 1.7 wt.% Ca, 0.2 wt.% K and 0.4 wt.% F; the sulphate concentration is 0.2 wt.% (Table 2). The charge balance reveals a significant excess of cations (33.3 %), which we attribute to dissolved bicarbonate ions (see below).

In contrast to Sample 7, Sample 11 is enriched in the LREE. Thus, for example, the Ce concentration is 15 ppm versus 2.1 ppm in Sample 7 (Table 2). Like Sample 7, however, the profile displays a strong negative Eu anomaly but shows a much stronger positive Sm anomaly (Fig. 4). The MREE (Sm to Er) are also more enriched in Sample 11 than Sample 7 (e.g., 12 vs. 1.3 ppm for Dy), whereas the opposite is true for HREE, particularly for Yb and Lu (Table 2). The content of Y, an HREE, however, is the highest of all the samples analysed (90 ppm). The total REE (TREE) concentration is 176 ppm.

Sample 13

Sample 13 only contains Group 2b inclusions, the aqueous component of which is dominated by Type IV inclusions. As the median salinity of these inclusions is 14 wt.% NaCl eq. (Vasyukova et al., 2016), the composition of the fluid extracted from Sample 13 was normalised to 8.4 wt.% Cl, the corresponding chlorinity. The major element composition of the normalised fluid is 5.0 wt.% Na, 0.3 wt.% Ca, 0.3 wt.% K and 0.2 wt.% F; the sulphate concentration is 0.6 wt.%

Vasyukova, O. V. and A. E. Williams-Jones. "Direct Measurement of Metal Concentrations in Fluid Inclusions, a Tale of Hydrothermal Alteration and Ree Ore Formation from Strange Lake, Canada." Chemical Geology 483 (Apr 20 2018): 385-96. http://dx.doi.org/10.1016/j.chemgeo.2018.03.003.

(Table 2). A charge balance calculation showed that the sum of the cations is only 4.3 % less than the sum anions, which is an excellent result that confirms the reliability of the analyses.

The chondrite-normalised REE profile for this sample is relatively flat from La to Nd, and displays a strong positive Sm anomaly, a strong negative Eu anomaly and a convex upward distribution in the MREE with a maximum at Dy (Fig. 4). Compared to Sample 11, the fluid from Sample 13 has considerably lower concentrations of all the REE except for Sc. Indeed, the Sc concentration is the highest of all the samples analysed (3 ppm, Table 2). The TREE content is 49 ppm (Table 2).

Pegmatite border

Sample 16 represents the unaltered border zone of the pegmatites, in which the major minerals are microcline, quartz and arfvedsonite (Fig. 3a), and contains only Group 2a inclusions, with the aqueous phase restricted to Type IV inclusions (Vasyukova et al., 2016). The analysed composition of the extracted fluid was normalised to 13.9 wt.% Cl, which corresponds to the median salinity of this fluid (23 wt.% NaCl eq; Vasyukova et al., 2016). The resulting major element composition of the fluid is 8.5 wt.% Na, 0.4 wt.% Ca, 0.5 wt.% K and 0.6 wt.% F; the sulphate concentration is 0.7 wt.% (Table 2). The sum of the cations is 5% less than that for the anions, and, as is the case for Sample 13, indicates excellent reliability of the analyses (Table 2).

The chondrite-normalised REE profile of the fluid from this sample is characterised by a strong negative Eu anomaly, a moderate enrichment in the LREE with concentrations very similar to those of Sample 11 (La to Pr), a modest depletion in the MREE (Gd to Dy) and a weak enrichment in the HREE (except Lu, Fig. 4). Unlike the preceding samples the behaviour of Sm is not anomalous. The scandium content is slightly lower than in Sample 13 (2.6 ppm vs. 3 ppm) but much higher than in the other samples. The TREE content is 64 ppm.

Quartz vein (Sample 2)

Like Sample 11, Sample 2 is dominated by Group 3 inclusions, but unlike Sample 11, the aqueous phase is restricted to Type V (aqueous-CO_2) inclusions (Vasyukova et al., 2016). The median salinity of these inclusions was determined to be 4 wt.% NaCl eq. (Vasyukova et al., 2016), and accordingly the composition of the fluid extracted from Sample 2 was normalised to 2.4 wt.% Cl, the corresponding chlorinity. The resulting major element composition is 2.5 wt.% Na, 0.2 wt.% Ca, 0.05 wt.% K and 0.1 wt.% F; the sulphate concentration is 0.1 wt.% (Table 2). As was the case for Sample 11, the charge balance for this sample revealed a significant excess

Vasyukova, O. V. and A. E. Williams-Jones. "Direct Measurement of Metal Concentrations in Fluid Inclusions, a Tale of Hydrothermal Alteration and Ree Ore Formation from Strange Lake, Canada." Chemical Geology 483 (Apr 20 2018): 385-96. http://dx.doi.org/10.1016/j.chemgeo.2018.03.003.

of cations over anions (21.7%), which we also consider to reflect the presence of bicarbonate ions (see below).

The REE content of Sample 2 is relatively high, i.e., the TREE content is 107 ppm (Table 2). The chondrite-normalised REE profile of Sample 2 is very similar in shape to that of Sample 13. However, although the two profiles are almost identical from La to Sm, the MREE convexity rises to higher concentrations than in Sample 13, and the maximum is at Er rather than Dy (Fig. 4). The yttrium content is the second highest (57 ppm) of the five samples (Table 2).

REE distribution in arfvedsonite, hematite and aegirine

As was mentioned above, arfvedsonite, hematite and aegirine were analysed for their major and trace element content. The latter two minerals replaced arfvedsonite pervasively over a wide area and in several stages; two generations of aegirine were recognised, early aegirine, which occurs as replacive rims on arfvedsonite (Fig. 5a), and late aegirine, which replaced the early aegirine and locally filled fractures in quartz (Fig. 5b). Three samples, namely Sample 204705, Sample BZ-10076-11 and Sample 2, were chosen for analysis and were selected to represent different stages and degrees of alteration (see the description of the samples in 'Samples' section above). The results of the analysis are presented in Table 4.

The chondrite-normalised REE profile for arfvedsonite (Sample 204705) is characterised by a relatively flat LREE distribution, a marked negative Eu anomaly and a strong HREE enrichment (Fig. 6). The early aegirine (Samples 204705 and BZ-10076-11) has a chondrite-normalised REE profile that is almost identical to that for arfvedsonite between La and Gd, but, in contrast to the arfvedsonite profile, the MREE display a concave distribution; the slope of the HREE distribution is steeper than that for arfvedsonite, with both profiles converging at Lu (Fig. 6). The chondrite-normalised REE profile for the late aegirine (Sample 2; Fig. 6) differs from that for the early aegirine, i.e., it is characterised by a positive LREE slope, a positive Sm anomaly, a strong negative Eu anomaly, a relatively flat MREE distribution and a modest enrichment in the HREE (Fig. 6).

Microscopic examination of the core from Samples 204705 and BZ-10076-11 showed that what appeared to be hematite macroscopically (Fig. 5c) is in fact aegirine containing finely-disseminated hematite (identified from their Fe content by SEM-EDS analyses) and at least one other mineral (Fig. 5d), which could not be identified due to the very small crystal size. The presence of small concentrations of fluorine, and concentrations of K and Zn that are elevated

Vasyukova, O. V. and A. E. Williams-Jones. "Direct Measurement of Metal Concentrations in Fluid Inclusions, a Tale of Hydrothermal Alteration and Ree Ore Formation from Strange Lake, Canada." Chemical Geology 483 (Apr 20 2018): 385-96. http://dx.doi.org/10.1016/j.chemgeo.2018.03.003.

relative to aegirine but depleted relative to arfvedsonite (Table 4), suggest that the unknown mineral may be relict arfvedsonite. Significantly, the chondrite-normalised REE profile of the aegirine containing finely-disseminated hematite is almost identical to that of the arfvedsonite but very different from the profile of either early or late aegirine (Fig. 6). The reason for this unusual behaviour of the hematite-associated aegirine is discussed later.

Discussion

The excess cation issue

A matter of some concern was the fact that for two of the samples (Sample 11 and Sample 2), the crush leach experiments reported analyses in which there was a considerable excess in the sum of cation charge over that for the anions. This suggests that there was an important anion(s) present, which was not analysed. We believe that this anion was HCO_3^- based on the observations that Samples 2 and 11 contain a high proportion of aqueous-CO_2 inclusions, that nahcolite was present in aqueous inclusions in Sample 11, and thermodynamic calculations of Vasyukova et al. (2016). The aqueous phase in these inclusions therefore would have been saturated in CO_2 and at the conditions of entrapment would have contained high concentrations of HCO_3^-.

Fluid Evolution and Progressive Mobilisation of the REE

Stage 1-2a (mobilisation of the LREE)

The Group 2a fluid inclusions (Sample 16) record the earliest hydrothermal activity that affected the pegmatites (Fig. 2). This fluid was trapped at relatively high temperature (425°C), and had high salinity (23 wt.% NaCl), with chloride the dominant anion and Na the dominant cation. As it was in equilibrium with primary magmatic minerals the fluid did not cause any alteration. We conclude that the pH was high, because of equilibration of the fluid with an assemblage comprising arfvedsonite, quartz, albite and microcline. Indeed, our calculations show that an aqueous fluid with a salinity 23 wt.% NaCl in equilibrium with this assemblage at 425 ^oC would have a pH of 10.1 (Table 6). The fluid has a chondrite-normalised REE profile almost identical in shape to that of the host granites (Fig. 4).

The concentrations of the REE in a fluid depend on the ability of the fluid to dissolve REE-bearing minerals, which depends, in turn, on its properties (pH, oxidation state, the activity of major ligands as well as on temperature and pressure conditions) and the availability of the REE

Vasyukova, O. V. and A. E. Williams-Jones. "Direct Measurement of Metal Concentrations in Fluid Inclusions, a Tale of Hydrothermal Alteration and Ree Ore Formation from Strange Lake, Canada." Chemical Geology 483 (Apr 20 2018): 385-96. http://dx.doi.org/10.1016/j.chemgeo.2018.03.003.

(the source). The greater enrichment in the LREE over the HREE in Fluid 2a is generally consistent with the conclusion from the experiments of Migdisov et al. (2009) that LREE chloride and fluoride complexes are much more stable at high temperature than the corresponding HREE complexes. It should be cautioned, however, that this conclusion applies only for low pH. Unfortunately there are no experimental data on REE chloride and fluoride complexes at high pH, and it has been shown that the theoretical data (Haas et al., 1995) greatly overestimate the stability of the HREE complexes and underestimate those of the LREE (Wood et al., 2002; Migdisov et al., 2009) at high temperature, albeit at low pH. From what is known for low pH, it is reasonable to assume that fluoride complexation will play an important role in REE solubility at high pH, particularly given the fact that HF is completely dissociated at these conditions. Indeed, unpublished data from a preliminary synchrotron experiment at 450 ^{o}C by the authors in collaboration with colleagues from Australia and France have revealed high concentrations of Sm (50 ppm) in a fluoride-bearing NaOH solution with a pH of 10; the Sm concentration of the Stage 1-2a fluid was 1.7 ppm (Table 2). This, and the extremely high fluoride content of the Stage 1-2a fluid (0.6 wt.%) make a strong case that fluoride ions played an important role in REE transport in the early evolution of the fluids at Strange Lake. We speculate, moreover, by analogy with what is known of the behaviour of Zr, Nb and Ta (Migdisov et al., 2011; Timofeev et al., 2015; Timofeev et al., 2017) that the causative species was a REE hydroxy-fluoride complex.

A potentially more important reason for the LREE enrichment of the Stage 1-2a fluid was the availability of a fluoride melt into which the LREE had partitioned preferentially (relative to silicate melt) and crystallised as primary LREE minerals (fluorbritholite-(Ce) and LREE-rich fluorite; Vasyukova and Williams-Jones, 2014). The Stage 1-2a fluid would readily have leached REE from this source, something that is suggested by the fact that the fluid extracted from Sample 16 has the highest F content of any of the extracted fluids analysed (Table 2). The low content of the HREE can be explained by the fact that these elements remained in the silicate melt and partitioned into minerals such as zirconosilicates and arfvedsonite (Siegel et al., 2017). The failure of these HREE-bearing minerals to decompose (the Stage 1-2a fluid was in equilibrium with these minerals; see above) and release the HREE therefore ensured that the Stage 1-2a fluid was not HREE-enriched.

Vasyukova, O. V. and A. E. Williams-Jones. "Direct Measurement of Metal Concentrations in Fluid Inclusions, a Tale of Hydrothermal Alteration and Ree Ore Formation from Strange Lake, Canada." Chemical Geology 483 (Apr 20 2018): 385-96. http://dx.doi.org/10.1016/j.chemgeo.2018.03.003.

Stage 2b-3 (mobilisation of the MREE)

As noted earlier, the Group 2b fluid is represented by fluid inclusions trapped in Sample 13 and records Stage 2b-3 of the hydrothermal system. This fluid was trapped at lower temperature, i.e., ~360°C, and has lower salinity (14 wt.% NaCl equivalent) than the Stage 1-2a fluid. Nonetheless, the system remained NaCl-dominated. The evolution of the fluid from Stage 1-2a to Stage 2b-3 was governed by gradual cooling and oxidation. This and the availability of Na^+ from the Stage 1-2a fluid caused alteration of arfvedsonite to aegirine according to the reaction:

$$(\text{Arf})\ Na_3Fe_5Si_8O_{22}(OH)_2 + (\text{Qtz})\ 2SiO_2 + O_2 + 2Na^+ = (\text{Aeg})\ 5NaFeSi_2O_6 + 2H^+ \qquad (1)$$

The alteration, in turn, reduced the salinity of the fluid and decreased pH (Vasyukova et al., 2016). Assuming that the fluid had a salinity of 14 wt.% NaCl and was in equilibrium with arfvedsonite, aegirine, quartz, albite and microcline at 360 ^oC, the pH would have been 9.7, i.e., it would have remained relatively high (Table 6).

The evolution of the hydrothermal system to Stage 2b-3 was accompanied by a large change in the distribution of the REE. The major difference was a decrease in the concentration of the LREE and a significant increase in the content of the MREE (Fig. 4); there was also a decrease in the concentrations of the HREE. We do not know exactly what affected the fluid at this stage, and due to a lack of experimental data for high pH fluids, it is not possible to model these changes. The following conditions changed compared to the previous stage: 1) temperature decreased; 2) salinity decreased; 3) the oxidation state increased; and 4) there was disequilibrium between the fluid and the surrounding rocks (alteration of arfvedsonite to aegirine). Based on the observation that early aegirine is depleted in the MREE relative to arfvedsonite (Fig. 6), we propose that this alteration released MREE to the fluid, nicely accounting for the convex nature of the MREE part of the profile of Sample 13 (Fig. 4). This alteration, however, cannot have been responsible for the depletion in the LREE content of the fluid (Sample 13, Fig. 4) relative to that of its predecessor (Sample 16, Fig. 4) because the LREE content of the early aegirine is almost the same as that of the arfvedsonite (Fig. 6a). We propose, instead, that this depletion in the LREE occurred because the lower temperature of this stage (360 °C) lead to the saturation of the fluid in LREE minerals, which removed LREE from the fluid. Based on the study of Gysi and Williams-Jones (2013), the most likely candidates for these minerals are fluocerite-(Ce) and LREE-rich fluorite. This interpretation is supported by the observation that the fluorine content of the Stage 2b-3 fluid is three times less than that of the Stage 1-2a fluid.

Vasyukova, O. V. and A. E. Williams-Jones. "Direct Measurement of Metal Concentrations in Fluid Inclusions, a Tale of Hydrothermal Alteration and Ree Ore Formation from Strange Lake, Canada." Chemical Geology 483 (Apr 20 2018): 385-96. http://dx.doi.org/10.1016/j.chemgeo.2018.03.003.

Further evolution of the fluid is evident from Samples 11 and 2, which represent early (nahcolite-rich) and late Stage 3 (CO_2-gas-saturated) fluids, respectively (Fig. 2). The fluid inclusions in these samples are HCO_3^--dominant, and contained roughly equal proportions of HCO_3^- and Cl^-, respectively (Table 2). Sample 11 provides evidence for a rapid change of pH during fluid entrapment (~250-300°C) in the form of: 1) inclusions with accidently trapped nahcolite; 2) inclusions crystallising nahcolite only upon cooling; and 3) inclusions with a CO_2 gas bubble (nahcolite did not crystallise even after cooling), all in a single inclusion assemblage. In pH-temperature (^oC) co-ordinates, such a fluid would have been trapped along the red dashed line (Fig. 7), i.e., from a pH of 9.4 at 300 ^oC to a pH of 3.2 at 250 ^oC. The lowest pH at this stage (3.2) corresponds to a fluid in equilibrium with quartz and saturated with CO_2 gas at 250°C (Table 6). This low pH, CO_2-saturated fluid represents the fluid population trapped in Sample 2.

The most probable reason for the precipitous drop in pH reported above was the termination of arfvedsonite alteration by Reaction 1, which occurred because the salinity of the fluid was insufficient for the reaction to proceed (less than 14 wt.% NaCl eq.). As a result of the associated change in fO_2 (see Vasyukova et al., 2016), the CH_4 was converted abruptly into CO_2, thereby decreasing pH. This CO_2-saturated, low pH fluid, was extremely reactive, and lead to further intense alteration of arfvedsonite via the reactions:

$$(Arf)\ Na_3Fe_5Si_8O_{22}(OH)_2 + O_2 + 3H^+ + 13.5H_2O = 2.5(Hem)Fe_2O_3 + 8H_4SiO_4^\circ + 3Na^+ \quad (2)$$

$$2(Arf)\ Na_3Fe_5Si_8O_{22}(OH)_2 + 2O_2 + 6H_2O = 6(Aeg)\ NaFeSi_2O_6 + 2(Hem)Fe_2O_3 + 4H_4SiO_4^\circ \quad (3)$$

The result of these reactions is particularly evident in the intense alteration halo surrounding the quartz vein, from which Sample 2 was taken, and in which arfvedsonite was completely replaced by aegirine (Fig. 3d). It is notable that although Sample 2 contains a CO_2-saturated fluid with low pH, which points to its later origin than the fluid from Sample 11, the shape of its chondrite-normalised REE profile is much closer to that of Sample 13 (Stage 2b) than to Sample 11 (Fig. 4). The LREE content is very similar to that in Sample 13, and there is convex distribution centred on the MREE, albeit to much higher concentrations (Fig. 4). As was the case for Sample 13, the REE composition of the fluid trapped in Sample 2 was strongly influenced by the replacement of arfvedsonite with aegirine (Fig. 3d), which released REE into the fluid. We propose that the similarity of the profiles (Samples 2 and 13) reflects the fact that the REE source was the same, i.e., decomposition of arfvedsonite. The difference, i.e., the higher level of the MREE and HREE enrichment in Sample 2, reflects a more advanced stage of arfvedsonite

Vasyukova, O. V. and A. E. Williams-Jones. "Direct Measurement of Metal Concentrations in Fluid Inclusions, a Tale of Hydrothermal Alteration and Ree Ore Formation from Strange Lake, Canada." Chemical Geology 483 (Apr 20 2018): 385-96. http://dx.doi.org/10.1016/j.chemgeo.2018.03.003.

alteration. This is because the more aggressive fluid from Sample 2 (lower pH) was able to alter more arfvedsonite and therefore promote the release of more REE (especially the MREE and HREE) into the fluid compared to the fluid extracted from Sample 13, which had a much higher pH and was not able to cause as much damage to the arfvedsonite.

Another reason for the enrichment of the fluid in the MREE at this stage could have been the alteration of primary REE minerals to bastnäsite-(Ce) promoted by the high content of CO_2. An example of this alteration was provided by Vasyukova and Williams-Jones (2016), who described the replacement of primary fluorbritholite-(Ce) by fluocerite-(Ce) and then by bastnäsite-(Ce) (see Figure 5d of Vasyukova and Williams-Jones, 2016). As the primary fluorbritholite-(Ce) contains 2.1 wt.% Sm_2O_3, 2.3 wt.% Gd_2O_3 and 3.1 wt.% Y_2O_3, and the secondary bastnäsite-(Ce) only contains 1.2, 0.6 and 0.2 wt.% Sm_2O_3, Gd_2O_3 and Y_2O_3, respectively, the replacement would have released appreciable amounts of Sm, Gd and Y.

The REE enrichment of Sample 11 is very similar to that of Sample 2, except that the LREE and HREE contents are higher (Fig. 4). As was shown earlier, the LREE content during Stage 2b-3 was buffered to a low level by precipitation of LREE-rich fluorite, fluocerite-(Ce) and bastnäsite-(Ce). We, therefore, consider the higher LREE concentrations in this sample to be evidence for the presence of inclusions other than Group 3 fluid inclusions, i.e., the Group 2a fluid. The higher HREE content of Sample 11 relative to Sample 2 probably reflects a transition towards the conditions responsible for Stage 4-5 of the fluid evolution, which was marked by strong HREE enrichment (see below).

Stage 4-5 (mobilisation of HREE)

Group 4 fluid inclusions, representing Stage 4 in the fluid evolution, were trapped at ~220°C, have relatively low salinity (~4-10 wt% NaCl eq.) and are CO_2-free (Fig. 2). This fluid is interpreted to have evolved from the Stage 3 fluid by further cooling and loss of CO_2-gas (Vasyukova et al., 2016). We propose that the starting composition for the Stage 4 fluid was the same as that for the aqueous component of the fluid from the previous stage, i.e., it had a salinity of 4 wt.% NaCl eq. The calculated pH for this fluid at 220 ^oC is 3.1 (Table 6). Its further evolution was governed by cooling and fluid-rock interaction, i.e., in the absence of CO_2 gas, pH was unbuffered and gradually increased due to reaction with Na-rich minerals. The salinity increased due to consumption of water to form phyllosilicates. Eventually, the Stage 4 fluid evolved to the Stage 5 fluid, which, at ~150^oC, had a salinity of ~19 wt% NaCl eq., and was at a pH of between ~5.3 and 6.2 (Table 6).

Vasyukova, O. V. and A. E. Williams-Jones. "Direct Measurement of Metal Concentrations in Fluid Inclusions, a Tale of Hydrothermal Alteration and Ree Ore Formation from Strange Lake, Canada." Chemical Geology 483 (Apr 20 2018): 385-96. http://dx.doi.org/10.1016/j.chemgeo.2018.03.003.

Sample 7, which comprises a mixture of Group 4 and 5 inclusions represents the Stage 4-5 fluid. The salinity of this fluid was estimated to be 10 wt.% NaCl eq. (see Results). Fluid from this stage is characterised by a LREE content similar to that of fluids extracted from Sample 13 (Stage 2b) and Sample 2 (Stage 3), and a low MREE content, whereas its HREE content increases sharply with increasing atomic number of the REE, and exceeds that of the other fluids for Yb and Lu (Fig. 4). We propose that the increase in the HREE at this stage was due in part to the higher stability of the HREE chlorides and fluorides at lower temperature (150 ^{o}C for this stage versus 250 ^{o}C for the previous stage). This conclusion comes from the experimental data of Migdisov and Williams-Jones (2007) and Migdisov et al. (2009), which showed that at ~ 150°C there is a switch in the relative stability of the LREE and HREE complexes. Whereas the LREE chloride and fluoride complexes are more stable than the HREE complexes above this temperature, the reverse is true at lower temperature. The REE content for the Stage 4-5 fluid was modelled using the thermodynamic data for fluoride and chloride complexes in Migdisov et al. (2009). Our calculations show that the fluid in Stage 4 (220 ^{o}C) contained 1.6 ppm Ce, 1 ppm Nd, 4.3 ppm Dy and 4.7 ppm Yb, whereas in Stage 5 (150 ^{o}C) the fluid only contained 0.08 ppm Ce, 0.07 ppm Nd, 1.9 ppm Dy and 26 ppm Yb (black and red dots in Fig. 8; Table 7). The calculated concentrations for Ce and Nd in Stage 4 are nearly identical to their measured concentrations, and the calculated concentrations for Dy and Yb in Stage 5 are very similar to the corresponding measured concentrations (Fig. 8). We, therefore, propose that the LREE in this sample were introduced mainly during Stage 4, and the HREE mainly during Stage 5.

Earlier, we noted that the evolution of the fluid during Stage 5 was driven by the interaction of the low pH Group 4 fluid with the surrounding rocks. This is especially evident from the massive hematisation (Fig. 3e), which was caused by alteration of arfvedsonite (Reactions 2 and 3). Both reactions are driven by oxidation, however, Reaction 2 is also pH-dependent and only can proceed at low pH. This suggests that the low pH fluid of Stage 4 promoted alteration of arfvedsonite to hematite, whereas the higher pH of the Stage 5 fluid lead to the alteration of arfvedsonite by aegirine and (finely disseminated) hematite (Fig. 6).

In theory, the switch from more stable LREE complexes to more stable HREE complexes at lower temperature during Stage 5 should have been accompanied by the precipitation of LREE and MREE-rich minerals. Indeed, as reported by Gysi et al. (2016), the alteration of arfvedsonite in the pegmatite was accompanied by the precipitation of LREE-enriched ferri-allanite-(Ce) and MREE-enriched gadolinite-(Y).

Vasyukova, O. V. and A. E. Williams-Jones. "Direct Measurement of Metal Concentrations in Fluid Inclusions, a Tale of Hydrothermal Alteration and Ree Ore Formation from Strange Lake, Canada."
Chemical Geology 483 (Apr 20 2018): 385-96. http://dx.doi.org/10.1016/j.chemgeo.2018.03.003.

Further cooling (below 150 ^{o}C) of the Stage 5 fluid eventually caused precipitation of HREE-enriched minerals or overgrowth of HREE-rich layers on existing REE minerals as shown by the occurrence of overgrowths of Y- and Yb-rich gadolinite-(Y) on Gd- and Dy-rich gadolinite-(Y) (Fig. 10 in Gysi et al., 2016).

A model for the Strange Lake Hydrothermal System

The onset of hydrothermal activity in the Strange Lake pegmatites occurred with the exsolution of an aqueous-carbonic fluid at ~450-500 °C and a pressure of 1.1 kbar (Stage 1). This fluid had a salinity of 25 wt.% NaCl eq. and was saturated with a CH_4+H_2 gas, reflecting an oxygen fugacity ~ 7 log units below that of the QFM buffer (Vasyukova et al., 2016). The fluid was in equilibrium with the host rocks (there is no evidence of hydrothermal alteration).

Evolution of the fluid occurred in a closed system, i.e., the pegmatites "stewed in their own juices", and was driven by cooling-induced oxidation and fluid-rock interaction. By that time the fluid had cooled to ~425 °C and the oxygen fugacity had increased to 6.2 log units below the QFM buffer (Vasyukova et al., 2016). The salinity was effectively unchanged, equilibrium with the host rocks was maintained and the pH was 10, i.e., the fluid was extremely alkaline. Analysis of fluid extracted from Sample 16, representing this Stage (1-2a), indicates that the REE concentrations were ~ 10 times chondrite, except for the LREE, which were enriched to levels reaching ~15-30 times chondrite. The shape of the REE profile is very similar to that of the bulk granite, although the absolute concentration is several orders of magnitude lower (Fig. 4). The similarity of the two profiles is consistent with close system evolution and indicates nearly identical partitioning of the different REE between the fluid and the melt.

Equilibrium of the fluid with the surrounding rocks was maintained until the system cooled to ~360 °C (Stage 2b), when oxidation converted the CH_4 to higher hydrocarbons, and promoted alteration of arfvedsonite by aegirine. This lead to dilution of the fluid (H_2O supplied by the breakdown of arfvedsonite) and a decrease in the salinity (~14 wt.% NaCl eq.). The oxygen fugacity increased to 2.8 log units below the QFM buffer (Vasyukova et al., 2016) but the pH was essentially unchanged. The LREE content of the fluid decreased to ~5 times chondrite (Sample 13), probably because the fluid had cooled sufficiently to saturate with fluocerite-(Ce) and LREE-rich fluorite, which removed LREE from the fluid. In contrast, concentrations of the MREE increased considerably, creating a convexity in the chondrite-normalised REE profile with a maximum at Dy corresponding to a concentration ~20 times that of chondrite. We attribute this increased concentration of the MREE to the fact that alteration of the arfvedsonite

Vasyukova, O. V. and A. E. Williams-Jones. "Direct Measurement of Metal Concentrations in Fluid Inclusions, a Tale of Hydrothermal Alteration and Ree Ore Formation from Strange Lake, Canada." Chemical Geology 483 (Apr 20 2018): 385-96. http://dx.doi.org/10.1016/j.chemgeo.2018.03.003.

to aegirine preferentially released MREE to the fluid as shown by the depletion of aegirine in these elements (Fig. 6).

Ongoing cooling (Stage 3) to 250-300 °C was accompanied by additional oxidation that converted the remaining CH_4 (and the higher hydrocarbons) to CO_2. This had a major effect on the pH, which decreased to ~3, leading to intense alteration of arfvedsonite and further dilution of the fluid (~4 wt.% NaCl eq.). The Stage 3 fluid had a very similar LREE content to that of the preceding stage and, like the latter, was characterised by a pronounced enrichment of the MREE leading to a similar convexity in its chondrite-normalised REE profile. The absolute concentrations of the MREE (and HREE), however, were higher, up to ~ 60 times greater than chondrite and the maximum was displaced to Er. We believe that these higher concentrations of the MREE (and HREE) reflect the much more intense nature of the aegirinisation of the arfvedsonite relative to that in Stage 2b.

Stage 4 began when the fluid had cooled to ~ 220 °C and CO_2 was lost to the system due to its migration out of the pegmatites. In the absence of CO_2, the pH gradually increased as a result of fluid-rock interaction and by the time that the fluid had cooled to ~150 °C, which marked the beginning of Stage 5, the pH was ~ 6. This increase in pH was accompanied by an increase in salinity (~ 19 wt.% NaCl eq.) due to the formation of phyllosilicates. Stage 5 was marked by a sharp change in the distribution of the REE. As in Stages 2a and 3, the LREE were strongly depleted due to the buffering effects of LREE mineral precipitation. In contrast to these stages, however, there was also a strong depletion in the MREE and a progressive increase in the concentration of the HREE with increasing atomic number of the REE, such that Yb has a concentration ~150 times that of chondrite. This depletion in LREE and MREE and strong HREE enrichment is satisfactorily explained by the experimentally observed switch from more stable LREE complexes to more stable HREE complexes at temperatures below 150 °C and the consequent saturation in the fluid of LREE-enriched ferri-allanite-(Ce) and MREE-enriched gadolinite-(Y).

In summary, the Strange Lake hydrothermal fluids evolved in a closed system and the evolution of the REE composition of the fluid during cooling was a direct result of the changes in pH that occurred in response to the progressive oxidation of an initially highly reducing aqueous-carbonic fluid. These changes (mainly a reduction in pH) lead to the alteration of arfvedsonite, which released MREE and HREE to the fluid. The other significant source for the MREE was fluorbritholite-(Ce), which crystallised from the fluoride melt and released MREE when it was

Vasyukova, O. V. and A. E. Williams-Jones. "Direct Measurement of Metal Concentrations in Fluid Inclusions, a Tale of Hydrothermal Alteration and Ree Ore Formation from Strange Lake, Canada." Chemical Geology 483 (Apr 20 2018): 385-96. http://dx.doi.org/10.1016/j.chemgeo.2018.03.003.

altered to bastnäsite-(Ce). The changes in pH (and temperature) also controlled the REE speciation of the fluid, with REE-hydroxy and -hydroxy-fluoride species dominating at high pH and REE-chloride species at low pH, and played a key role in the overall fractionation of the different REE. This study emphasises the need for further analyses of the trace element chemistry of fluid inclusions in order to understand the complexity of the hydrothermal processes that can lead to the formation of major rare earth element deposits.

Acknowledgments

The research presented in this manuscript was funded by a grant from Quest Rare Minerals Ltd, a matching NSERC Collaborative Research and Development Grant and a NSERC Discovery Grant. Vincent van Hinsberg provided valuable advice on sample preparation and analysis, and Anna Jung, Isabelle Richer and Lang Shi assisted in the ICP-MS, AA and EMP analyses, respectively. Dr. Dirk Kirste of Simon Fraser University performed the IC analyses. Our student volunteer, Anna Migdisova, helped with the sample preparation.

Captions

Figure 1. A geological map of the Strange Lake pluton showing the distribution of the principal rock types and the locations of the samples, on which this study was based.

Figure 2. A chart summarising compositional and physicochemical data on the fluids associated with wall-rock alteration of the Strange Lake granites and pegmatites. The information was taken from Vasyukova et al. (2016). The numbers immediately below the arrow refer to log units of fO_2 relative to the QFM buffer.

Figure 3. Photographs of the samples on which this study was based. (a) Sample 16, the relatively unaltered border zone of a pegmatite cutting unaltered transsolvus granite, (b) Sample 13, a weakly altered border zone pegmatite, (c) Sample 11, the quartz-rich core of a strongly altered pegmatite, (d) Sample 2, a quartz vein cutting hypersolvus granite, (e) Sample 7, the quartz-rich core of a strongly hematised pegmatite. Qtz – quartz, Fsp – feldspar, Elp – elpidite, Hem – hematite, Arf – arfvedsonite, Aeg(E) – early aegirine, Aeg(L) – late aegirine in a quartz vein, Fl – fluorite, Pseud – pseudomorphs after alkali-zircono(titano)silicates.

Vasyukova, O. V. and A. E. Williams-Jones. "Direct Measurement of Metal Concentrations in Fluid Inclusions, a Tale of Hydrothermal Alteration and Ree Ore Formation from Strange Lake, Canada." Chemical Geology 483 (Apr 20 2018): 385-96. http://dx.doi.org/10.1016/j.chemgeo.2018.03.003.

Figure 4. Chondrite-normalised REE profiles for samples 2, 7, 11, 13 and 16. Also shown on the diagram are chondrite-normalised REE profiles for hypersolvus granite (HYP), transsolvus granite (TS) and pegmatite (PEG).

Figure 5. (a) A backscattered SEM image showing arfvedsonite replaced by early aegirine in the rim and partially hematised in the core. (b) A backscattered SEM image showing late aegirine, accompanied by minor kainosite-(Y), filling fractures in quartz. (c) An image taken with a stereoscopic microscope showing arfvedsonite (black), which was partially hematised (brown). Note that areas that appear to be hematite macroscopically are in fact aegirine containing finely disseminated hematite. The dashed rectangular indicates the location of image (d). (d) A backscattered SEM image enlarged from (c) showing aegirine (dark grey), a finely disseminated unknown mineral (light grey) and finely disseminated hematite (white). Qtz – quartz, Hem – hematite, Arf – arfvedsonite, Arf(H) – hematised arfvedsonite, Aeg(E) – early aegirine, Aeg(L) – late aegirine in a quartz vein, Aeg(H) – aegirine containing finely disseminated hematite, Kai – kainosite, UnM – an unidentified mineral.

Figure 6. Chondrite-normalised REE profiles for arfvedsonite (Arf), early aegirine (Aeg(E)), late aegirine (Aeg(L)) and aegirine containing finely disseminated hematite (Aeg(H)).

Figure 7. A pH-T diagram showing the path (red dashed line) for the Stage 3 Strange Lake fluid modified from Vasyukova et al. (2016). The blue and orange areas represent the stability fields for nahcolite and CO_2-gas, respectively. 1 – the field for fluid inclusions containing accidentally trapped nahcolite, 2 – the field for fluid inclusions, which crystallised nahcolite upon cooling, and 3 – the field for fluid inclusions, which did not crystallise nahcolite but contain CO_2-gas.

Figure 8. A chondrite-normalised REE diagram showing a profile for the Stage 4-5 fluid. Also shown are the thermodynamically calculated concentrations of Ce, Nd, Dy and Yb for this fluid at 150 ^{o}C (red dots) and 220 ^{o}C (black dots). See text for further detail.

References

Audetat, A., Gunther, D., Heinrich, C.A., 1998. Formation of a magmatic-hydrothermal ore deposit: Insights with LA-ICP-MS analysis of fluid inclusions. Science, 279(5359): 2091-2094.

Vasyukova, O. V. and A. E. Williams-Jones. "Direct Measurement of Metal Concentrations in Fluid Inclusions, a Tale of Hydrothermal Alteration and Ree Ore Formation from Strange Lake, Canada." Chemical Geology 483 (Apr 20 2018): 385-96. http://dx.doi.org/10.1016/j.chemgeo.2018.03.003.

Banks, D.A., Yardley, B.W.D., 1992. Crush-leach analysis of fluid inclusions in small natural and synthetic samples. Geochimica Et Cosmochimica Acta, 56(1): 245-248.

Banks, D.A., Yardley, B.W.D., Campbell, A.R., Jarvis, K.E., 1994. REE composition of an aqueous magmatic fluid - a fluid inclusion study from the Capitan pluton, New-Mexico, USA. Chemical Geology, 113(3-4): 259-272.

Bottrell, S.H., Yardley, B., Buckley, F., 1988. A modified crush-leach method for the analysis of fluid inclusion electrolytes. Bulletin De Mineralogie, 111(3-4): 279-290.

Bühn, B., Rankin, A.H., 1999. Composition of natural, volatile-rich Na-Ca-REE-Sr carbonatitic fluids trapped in fluid inclusions. Geochimica Et Cosmochimica Acta, 63(22): 3781-3797.

Bühn, B., Rankin, A.H., Schneider, J., Dulski, P., 2002. The nature of orthomagmatic, carbonatitic fluids precipitating REE,Sr-rich fluorite: fluid-inclusion evidence from the Okorusu fluorite deposit, Namibia. Chemical Geology, 186(1-2): 75-98.

Craig, J.R., Vaughan, D.J., 1994. Paragenesis, formation conditions, and fluid inclusion geothermometry of ores, Ore microscopy and ore petrography. John Willey & Sons, Inc., New York / Chichester / Brisbane / Toronto / Singapore, pp. 164-208.

Ghazi, A.M., Vanko, D.A., Roedder, E., Seeley, R.C., 1993. Determination of rare-earth elements in fluid Iinclusions by inductively-coupled plasma-mass spectrometry (ICP-MS). Geochimica Et Cosmochimica Acta, 57(18): 4513-4516.

Gysi, A.P., Williams-Jones, A.E., 2013. Hydrothermal mobilization of pegmatite-hosted REE and Zr at Strange Lake, Canada: A reaction path model. Geochimica et Cosmochimica Acta, 122: 324-352.

Gysi, A.P., Williams-Jones, A.E., Collins, P., 2016. Lithogeochemical vectors for hydrothermal processes in the Strange Lake peralkaline granitic REE-Zr-Nb deposit. Economic Geology, 111: 1241-1276.

Haas, J.R., Shock, E.L., Sassani, D.C., 1995. Rare-earth elements in hydrothermal systems - estimates of standard partial molal thermodynamic properties of aqueous complexes of the rare-earth elements at high pressures and temperatures. Geochimica Et Cosmochimica Acta, 59(21): 4329-4350.

Heinrich, C.A., 2007. Fluid-fluid interactions in magmatic-hydrothermal ore formation. Fluid-Fluid Interactions, 65: 363-387.

Longerich, H., 2008. Laser ablation–inductively coupled plasma–mass spectrometry (LA–ICP–MS); an introduction. In: Sylvester, P. (Ed.), Laser ablation ICP-MS in the Earth

Vasyukova, O. V. and A. E. Williams-Jones. "Direct Measurement of Metal Concentrations in Fluid Inclusions, a Tale of Hydrothermal Alteration and Ree Ore Formation from Strange Lake, Canada."
Chemical Geology 483 (Apr 20 2018): 385-96. http://dx.doi.org/10.1016/j.chemgeo.2018.03.003.

740 Sciences: Current practices and outstanding issues. Short Course Series. Short Course
741 Series Mineralogial Association of Canada.

742 Migdisov, A.A., Williams-Jones, A.E., 2007. An experimental study of the solubility and
743 speciation of neodymium (III) fluoride in F-bearing aqueous solutions. Geochimica Et
744 Cosmochimica Acta, 71(12): 3056-3069.

745 Migdisov, A.A., Williams-Jones, A.E., van Hinsberg, V., Salvi, S., 2011. An experimental study
746 of the solubility of baddeleyite (ZrO_2) in fluoride-bearing solutions at elevated
747 temperature. Geochimica Et Cosmochimica Acta, 75(23): 7426-7434.

748 Migdisov, A.A., Williams-Jones, A.E., Wagner, T., 2009. An experimental study of the
749 solubility and speciation of the Rare Earth Elements (III) in fluoride- and chloride-
750 bearing aqueous solutions at temperatures up to 300 degrees C. Geochimica Et
751 Cosmochimica Acta, 73(23): 7087-7109.

752 Miller, R.R., Heaman, L.M., Birkett, T.C., 1997. U-Pb zircon age of the Strange Lake
753 peralkaline complex: Implications for Mesoproterozoic peralkaline magmatism in north-
754 central Labrador. Precambrian Research, 81(1-2): 67-82.

755 Nassif, J.G., 1993. The Strange Lake peralkaline complex, Quebec-Labrador: The hypersolvus-
756 subsolvus granite transition and feldspar mineralogy, McGill University, Montreal, 104
757 pp.

758 Norman, D.I., Kyle, P.R., Baron, C., 1989. Analysis of trace-elements including rare-earth
759 elements in fluid inclusion liquids. Economic Geology, 84(1): 162-166.

760 Pettke, T., 2008. Analytical protocols for element concentration and isotope ratio measurements
761 in fluid inclusions by LA-(MC)-ICP-MS. In: Sylvester, P. (Ed.), Laser ablation ICP-MS
762 in the Earth Sciences: Current practices and outstanding issues. Short Course Series.
763 Short Course Series Mineralogial Association of Canada.

764 Roedder, E., 1977. Fluid inclusions as tools in mineral exploration. Economic Geology, 72: 503-
765 525.

766 Roedder, E. (Ed.), 1984. Fluid Inclusions. Reviews in Mineralogy, 12, 1-646.

767 Roedder, E., 1997. Fluid inclusion studies of hydrothermal ore deposits. In: Barnes, H.L. (Ed.),
768 Geochemistry of Hydrothermal Ore Deposits. Wiley, New York, pp. 657-697.

769 Shepherd, T.J., Chenery, S.R., 1995. Laser-Ablation ICP-MS elemental analysis of individual
770 fluid inclusions - an evaluation study. Geochimica Et Cosmochimica Acta, 59(19): 3997-
771 4007.

Vasyukova, O. V. and A. E. Williams-Jones. "Direct Measurement of Metal Concentrations in Fluid Inclusions,
a Tale of Hydrothermal Alteration and Ree Ore Formation from Strange Lake, Canada."
Chemical Geology 483 (Apr 20 2018): 385-96. http://dx.doi.org/10.1016/j.chemgeo.2018.03.003.

772 Shvarov, Y.V., 1999. Algorithmization of the numeric equilibrium modeling of dynamic
773 geochemical processes. Geokhimiya(6): 646-652.

774 Shvarov, Y.V., Bastrakov, E.N., 1999. HCh: a software package for geochemical equilibrium
775 modelling. User's Guide., Record 1999/25. Australian Geological Survey Organisation,
776 Record 1999/25, 61 pp.

777 Siegel, K., Williams-Jones, A.E., van Hinsberg, V.J., 2017. The amphiboles of the REE-rich A-
778 type peralkaline Strange Lake pluton – fingerprints of magma evolution. Lithos, 288-289:
779 156-174.

780 Skinner, B.J., 1979. The many origins of hydrothermal mineral deposits. In: Barnes, H.L. (Ed.),
781 Geochemistry of Hydrothermal Ore Deposits. Wiley & Sons, New York, NY, pp. 1-21.

782 Skinner, B.J., Barton, P.B., 1973. Genesis of mineral deposits. Annual Review of Earth and
783 Planetary Sciences, 1: 183-211.

784 Timofeev, A., Migdisov, A.A., Williams-Jones, A.E., 2015. An experimental study of the
785 solubility and speciation of niobium in fluoride-bearing aqueous solutions at elevated
786 temperature. Geochimica Et Cosmochimica Acta, 158: 103-111.

787 Timofeev, A., Migdisov, A.A., Williams-Jones, A.E., 2017. An experimental study of the
788 solubility and speciation of tantalum in fluoride-bearing aqueous solutions at elevated
789 temperature. Geochimica et Cosmochimica Acta, 197: 294-304.

790 Vasyukova, O.V., Williams-Jones, A.E., Blamey, N.J.F., 2016. Fluid evolution in the Strange
791 Lake granitic pluton, Canada: Implications for HFSE mobilisation. Chemical Geology,
792 444: 83-100.

793 Wilkinson, J.J., 2001. Fluid inclusions in hydrothermal ore deposits. Lithos, 55(1-4): 229-272.

794 Wood, S.A., Palmer, D.A., Wesolowski, D.J., Benezeth, P., 2002. The aqueous geochemistry of
795 the rare earth elements and yttrium. Part XI. The solubility of $Nd(OH)_3$ and hydrolysis of
796 Nd^{3+} from 30 to 290 °C at saturated water vapor pressure with in-situ pH_m measurement.
797 In: Hellmann, R., Wood, S.A. (Eds.), Water–rock interactions, ore deposits, and
798 environmental geochemistry: a tribute to David A. Crerar, Geochemical Society Special
799 Publication, pp. 229-256.

800

801

Vasyukova, O. V. and A. E. Williams-Jones. "Direct Measurement of Metal Concentrations in Fluid Inclusions,
a Tale of Hydrothermal Alteration and Ree Ore Formation from Strange Lake, Canada."
Chemical Geology 483 (Apr 20 2018): 385-96. http://dx.doi.org/10.1016/j.chemgeo.2018.03.003.

Figures

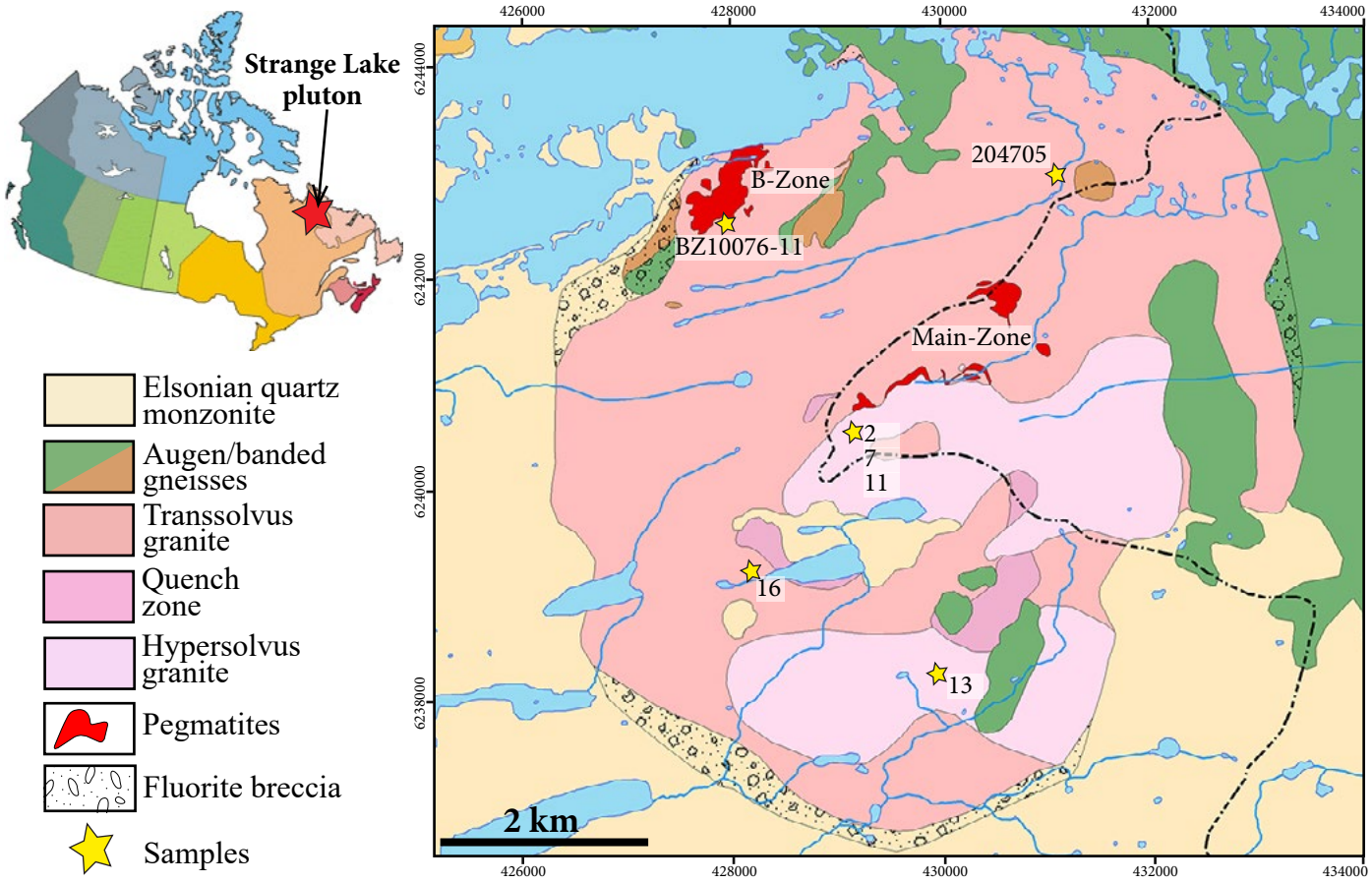

Figure 1 A geological map of the Strange Lake pluton showing the distribution of the principal rock types and the locations of the samples, on which this study was based.

Vasyukova, O. V. and A. E. Williams-Jones. "Direct Measurement of Metal Concentrations in Fluid Inclusions, a Tale of Hydrothermal Alteration and Ree Ore Formation from Strange Lake, Canada." Chemical Geology 483 (Apr 20 2018): 385-96. http://dx.doi.org/10.1016/j.chemgeo.2018.03.003.

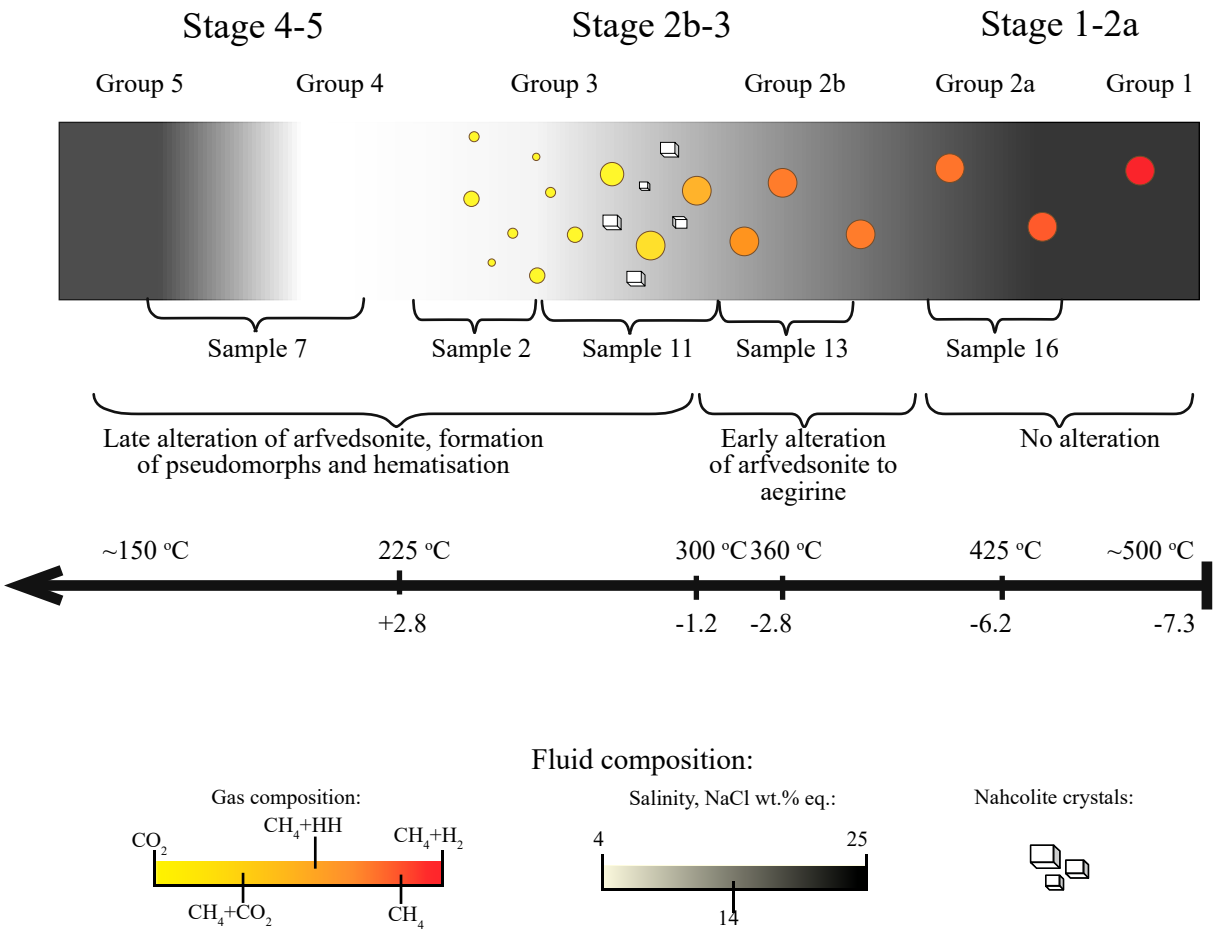

Figure 2 A chart summarising compositional and physicochemical data on the fluids associated with wall-rock alteration of the Strange Lake granites and pegmatites. The information was taken from Vasyukova et al. (2016). The numbers immediately below the arrow refer to log units of fO_2 relative to the QFM buffer.

Vasyukova, O. V. and A. E. Williams-Jones. "Direct Measurement of Metal Concentrations in Fluid Inclusions, a Tale of Hydrothermal Alteration and Ree Ore Formation from Strange Lake, Canada." Chemical Geology 483 (Apr 20 2018): 385-96. http://dx.doi.org/10.1016/j.chemgeo.2018.03.003.

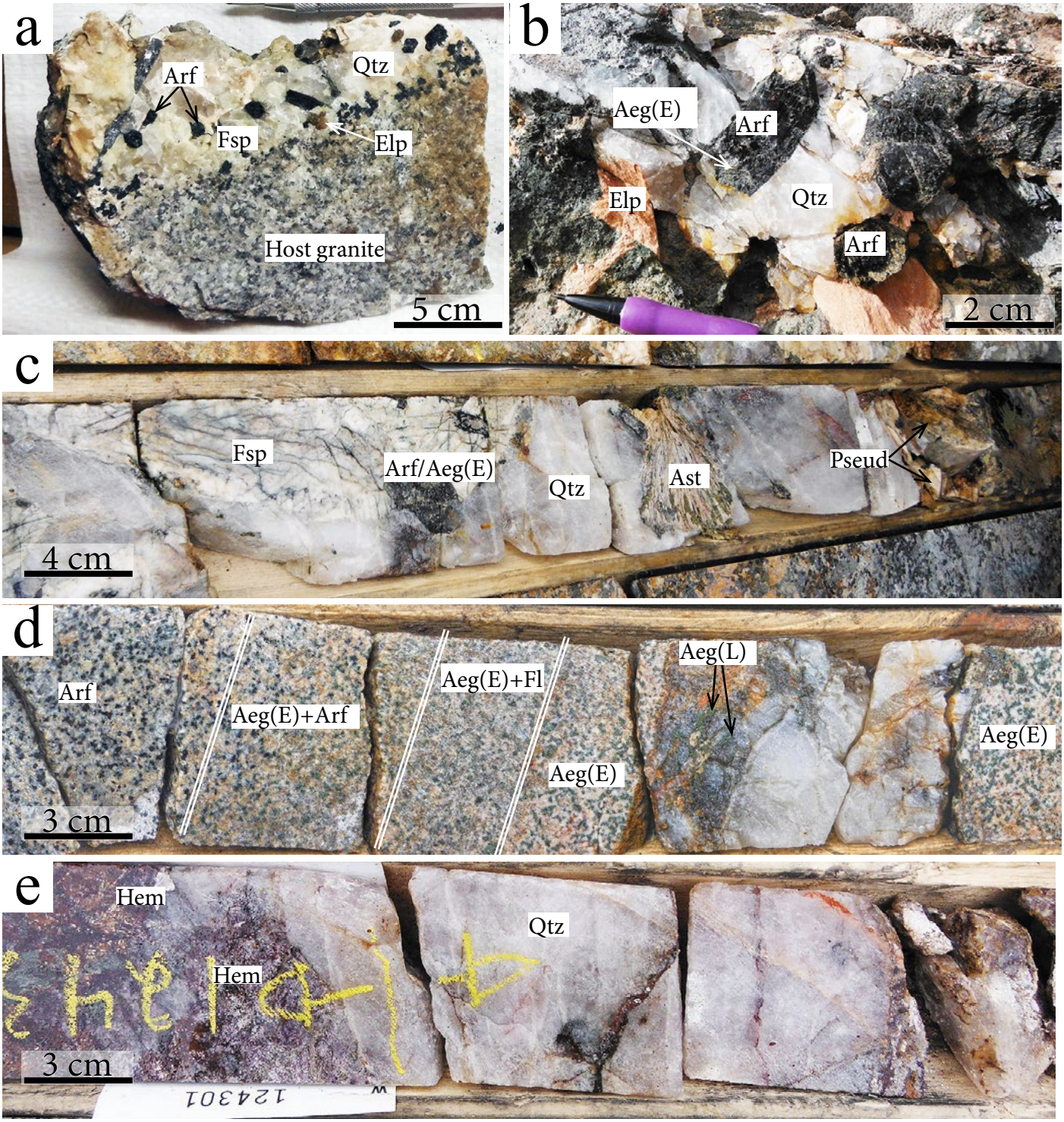

Figure 3 Photographs of the samples on which this study was based. (a) Sample 16, the relatively unaltered border zone of a pegmatite cutting unaltered transsolvus granite, (b) Sample 13, a weakly altered border zone pegmatite, (c) Sample 11, the quartz-rich core of a strongly altered pegmatite, (d) Sample 2, a quartz vein cutting hypersolvus granite, (e) Sample 7, the quartz-rich core of a strongly hematised pegmatite. Qtz – quartz, Fsp – feldspar, Elp – elpidite, Hem – hematite, Arf – arfvedsonite, Aeg(E) – early aegirine, Aeg(L) – late aegirine in a quartz vein, Fl – fluorite, Pseud – pseudomorphs after alkali-zircono(titano)silicates.

Vasyukova, O. V. and A. E. Williams-Jones. "Direct Measurement of Metal Concentrations in Fluid Inclusions, a Tale of Hydrothermal Alteration and Ree Ore Formation from Strange Lake, Canada." Chemical Geology 483 (Apr 20 2018): 385-96. http://dx.doi.org/10.1016/j.chemgeo.2018.03.003.

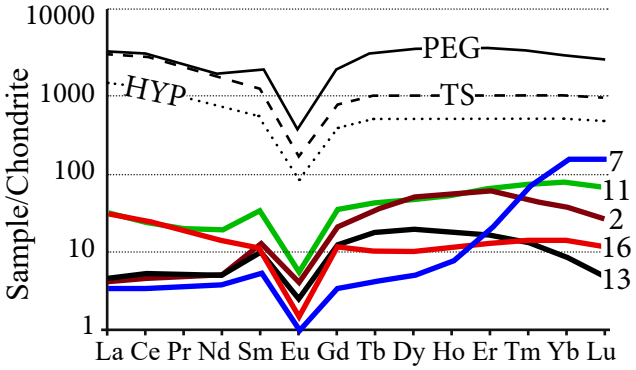

Figure 4 Chondrite-normalised REE profiles for samples 2, 7, 11, 13 and 16. Also shown on the diagram are chondrite-normalised REE profiles for hypersolvus granite (HYP), transsolvus granite (TS) and pegmatite (PEG).

Vasyukova, O. V. and A. E. Williams-Jones. "Direct Measurement of Metal Concentrations in Fluid Inclusions, a Tale of Hydrothermal Alteration and Ree Ore Formation from Strange Lake, Canada." Chemical Geology 483 (Apr 20 2018): 385-96. http://dx.doi.org/10.1016/j.chemgeo.2018.03.003.

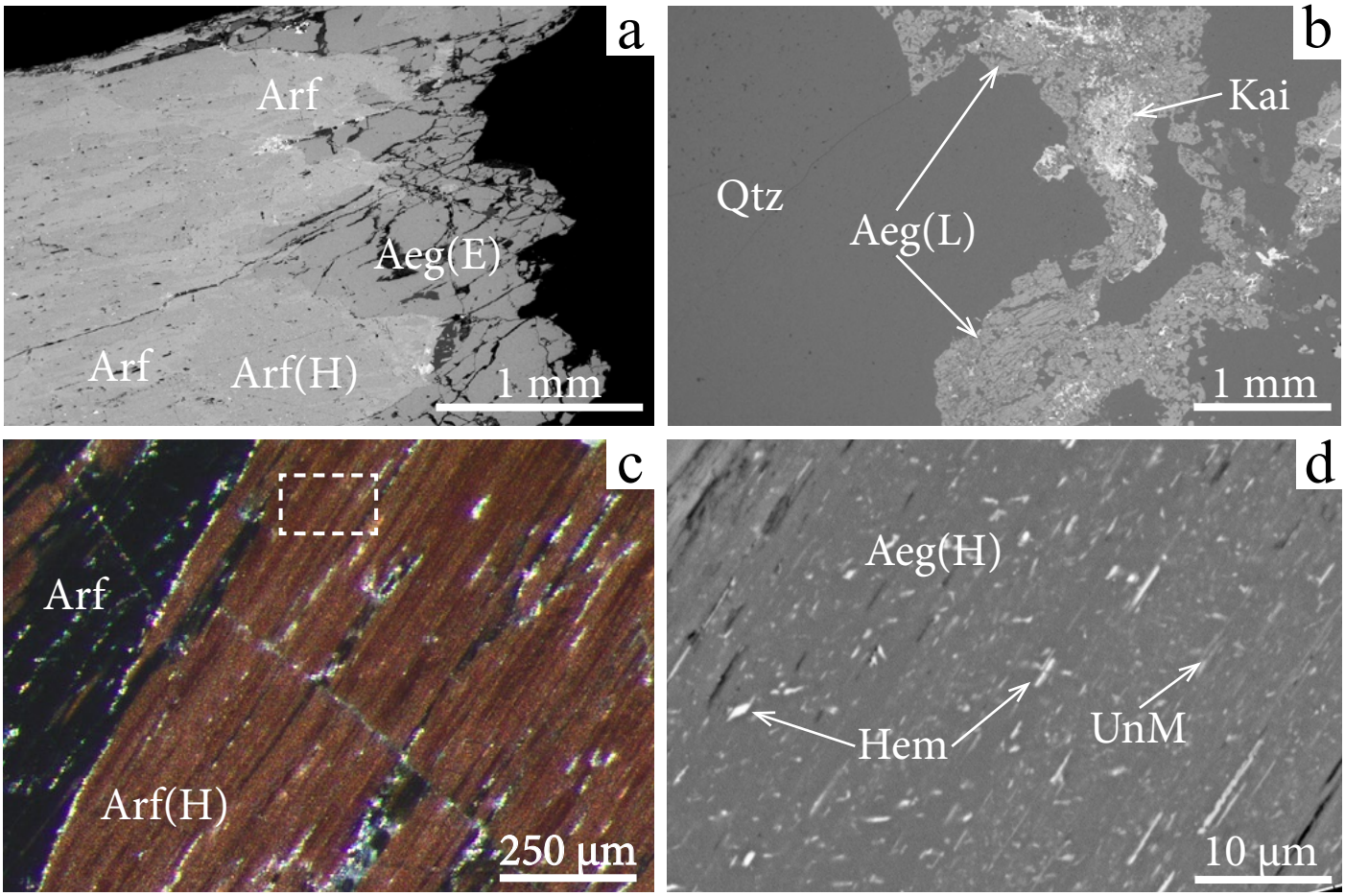

Figure 5 (a) A backscattered SEM image showing arfvedsonite replaced by early aegirine in the rim and partially hematised in the core. (b) A backscattered SEM image showing late aegirine, accompanied by minor kainosite-(Y), filling fractures in quartz. (c) An image taken with a stereoscopic microscope showing arfvedsonite (black), which was partially hematised (brown). Note that areas that appear to be hematite macroscopically are in fact aegirine containing finely disseminated hematite. The dashed rectangular indicates the location of image (d). (d) A backscattered SEM image enlarged from (c) showing aegirine (dark grey), a finely disseminated unknown mineral (light grey) and finely disseminated hematite (white). Qtz – quartz, Hem – hematite, Arf – arfvedsonite, Arf(H) – hematised arfvedsonite, Aeg(E) – early aegirine, Aeg(L) – late aegirine in a quartz vein, Aeg(H) – aegirine containing finely disseminated hematite, Kai – kainosite, UnM – an unidentified mineral.

Vasyukova, O. V. and A. E. Williams-Jones. "Direct Measurement of Metal Concentrations in Fluid Inclusions, a Tale of Hydrothermal Alteration and Ree Ore Formation from Strange Lake, Canada." Chemical Geology 483 (Apr 20 2018): 385-96. http://dx.doi.org/10.1016/j.chemgeo.2018.03.003.

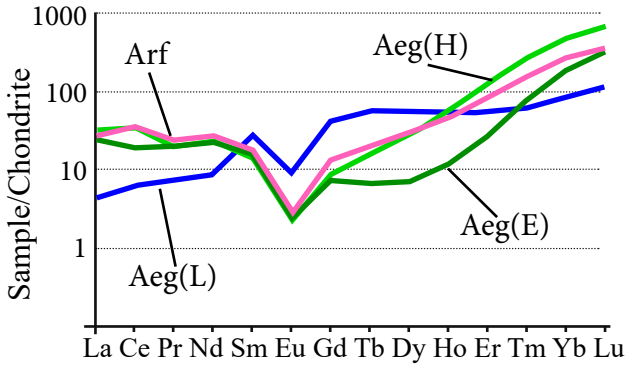

Figure 6 Chondrite-normalised REE profiles for arfvedsonite (Arf), early aegirine (Aeg(E)), late aegirine (Aeg(L)) and aegirine containing finely disseminated hematite (Aeg(H)).

Vasyukova, O. V. and A. E. Williams-Jones. "Direct Measurement of Metal Concentrations in Fluid Inclusions, a Tale of Hydrothermal Alteration and Ree Ore Formation from Strange Lake, Canada." Chemical Geology 483 (Apr 20 2018): 385-96. http://dx.doi.org/10.1016/j.chemgeo.2018.03.003.

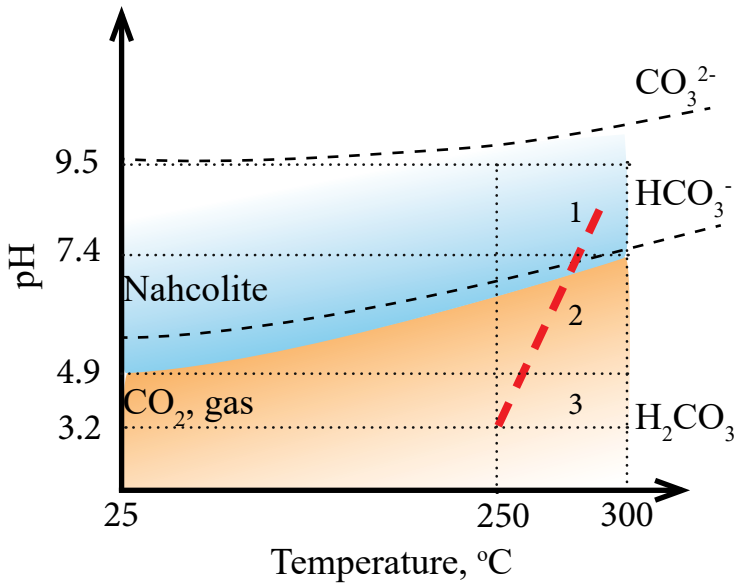

Figure 7 A pH-T diagram showing the path (red dashed line) for the Stage 3 Strange Lake fluid modified from Vasyukova et al. (2016). The blue and orange areas represent the stability fields for nahcolite and CO_2-gas, respectively. 1 – the field for fluid inclusions containing accidentally trapped nahcolite, 2 – the field for fluid inclusions, which crystallised nahcolite upon cooling, and 3 – the field for fluid inclusions, which did not crystallise nahcolite but contain CO_2-gas.

Vasyukova, O. V. and A. E. Williams-Jones. "Direct Measurement of Metal Concentrations in Fluid Inclusions, a Tale of Hydrothermal Alteration and Ree Ore Formation from Strange Lake, Canada." Chemical Geology 483 (Apr 20 2018): 385-96. http://dx.doi.org/10.1016/j.chemgeo.2018.03.003.

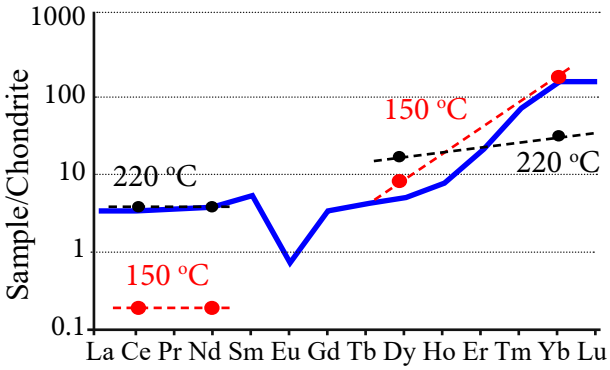

Figure 8 A chondrite-normalised REE diagram showing a profile for the Stage 4-5 fluid. Also shown are the thermodynamically calculated concentrations of Ce, Nd, Dy and Yb for this fluid at 150 °C (red dots) and 220 °C (black dots). See text for further detail.

Vasyukova, O. V. and A. E. Williams-Jones. "Direct Measurement of Metal Concentrations in Fluid Inclusions, a Tale of Hydrothermal Alteration and Ree Ore Formation from Strange Lake, Canada." Chemical Geology 483 (Apr 20 2018): 385-96. http://dx.doi.org/10.1016/j.chemgeo.2018.03.003.

Tables

Click here to download Table: CrushLeach_Tables.docx

Table 1 Composition of the leachate fluids analysed using ICP-MS.

ppb	[4]Detection limits	PB-1	2	7	11	13	16	PB-2
[1]Na	4.7	166	8,241	2,771	5,240	3,138	2,385	39
[2]Ca	100	116	556	530	2,434	158	101	103
K	22	bdl	186	82	273	155	151	bdl
Fe	6.3	12	31	14	26	bdl	17	bdl
Li	0.06	0.2	30	23	75	8.5	0.6	0.4
[3]Cl	100	bdl	7,992	6,082	5,096	5,205	3,887	bdl
[3]F	5	bdl	377	51	510	137	179	29
[3]SO_4	20	bdl	343	196	306	390	209	84
Y	0.0004	0.03	19	0.8	13	1.5	0.6	0.04
La	0.0006	0.07	0.3	0.09	1	0.06	0.2	0.1
Ce	0.002	0.08	1	0.2	2.1	0.2	0.4	0.2
Pr	0.0002	0.009	0.2	0.04	0.3	0.03	0.05	0.002
Nd	0.0003	0.03	0.8	0.2	1.2	0.1	0.2	0.02
Sm	0.0004	0.003	0.7	0.08	0.6	0.09	0.06	0.003
Eu	0.0004	0.0007	0.08	0.005	0.04	0.008	0.004	0.001
Gd	0.0003	0.01	1.5	0.07	1.1	0.2	0.08	0.03
Tb	0.0003	0.0007	0.5	0.02	0.2	0.04	0.01	0.001
Dy	0.0004	0.002	4.2	0.1	1.7	0.3	0.07	0.006
Ho	0.0001	0.001	1	0.04	0.4	0.06	0.02	0.002
Er	0.0003	0.002	3.1	0.3	1.4	0.2	0.06	0.005
Tm	0.0001	0.0003	0.4	0.2	0.2	0.02	0.01	0.0009
Yb	0.0002	0.001	2.3	2.4	1.6	0.08	0.08	0.007
Lu	0.0002	0.0003	0.2	0.4	0.2	0.007	0.01	0.002

PB1andPB2 – procedure blanks
bdl – below detection limit
[1] – analysed from solutions made for IC (ultrapure water as a leaching solution)
[2] – analysed by AA
[3] – analysed by IC
[4] – concentrations in the leaching solution were taken as the detection limits except for F, Cl and SO_4 for which detection limits were calculated from IC calibration curves

Vasyukova, O. V. and A. E. Williams-Jones. "Direct Measurement of Metal Concentrations in Fluid Inclusions, a Tale of Hydrothermal Alteration and Ree Ore Formation from Strange Lake, Canada."
Chemical Geology 483 (Apr 20 2018): 385-96. http://dx.doi.org/10.1016/j.chemgeo.2018.03.003.

Table 2 Composition of the fluids normalised to salinity (from fluid inclusion microthermometric data).

ppm	2	7	11	13	16
Na	24,889	27,490	37,231	50,924	85,184
Ca	1,680	5,263	17,295	2,567	3,608
K	561	816	1,937	2,511	5,396
Fe	94	135	183	101	122
Li	90	228	536	138	29
Zn	98	189	98	413	387
Cl	24,138	60,345	36,207	84,483	138,790
F	1,138	506	3,621	2,218	6,406
SO_4	1,034	1,947	2,172	6,336	7,473
*HCO_3	26,137		77,679		
Sc	0.5	0.5	0.5	3.0	2.6
Y	57	7.6	90	24	16
La	1	0.9	7.2	1	7.4
Ce	2.9	2.1	15	3	16
Pr	0.5	0.4	2	0.5	1.9
Nd	2.5	1.7	8.9	2.2	6.6
Sm	2.1	0.8	4.5	1.5	1.7
Eu	0.2	0.05	0.3	0.1	0.1
Gd	4.7	0.7	7.5	2.5	2.5
Tb	1.5	0.2	1.6	0.7	0.4
Dy	13	1.3	12	5	2.7
Ho	2.9	0.4	2.9	1	0.6
Er	9.3	3.2	9.8	2.7	2.2
Tm	1.3	1.6	1.7	0.3	0.4
Yb	7	24	11	1.4	2.3
Lu	0.7	3.9	1.4	0.1	0.3
TREE	107	49	176	49	64
Salinity	4	10	6	14	23
Charge balance (total cations-total anions), %	21.7	-8.8	33.3	-4.3	-4.9

* - calculated from charge balance

Vasyukova, O. V. and A. E. Williams-Jones. "Direct Measurement of Metal Concentrations in Fluid Inclusions, a Tale of Hydrothermal Alteration and Ree Ore Formation from Strange Lake, Canada." Chemical Geology 483 (Apr 20 2018): 385-96. http://dx.doi.org/10.1016/j.chemgeo.2018.03.003.

Table 3 Standards, counting times and detection limits for EMP analysis.

Element	Standard	Counting time, sec	Detection limits, ppm
Al	Orthoclase	20	211
Ca	Diopside	20	237
F	Fluorite	100	2404
Fe	Hematite	20	270
K	Orthoclase	20	210
Mg	Diopside	20	213
Mn	Spessartine	20	270
Na	Albite	20	252
Si	Diopside	20	356
Ti	Rutile	20	368
Zn	Willemite	20	406
Zr	Zircon	20	821

Vasyukova, O. V. and A. E. Williams-Jones. "Direct Measurement of Metal Concentrations in Fluid Inclusions, a Tale of Hydrothermal Alteration and Ree Ore Formation from Strange Lake, Canada." Chemical Geology 483 (Apr 20 2018): 385-96. http://dx.doi.org/10.1016/j.chemgeo.2018.03.003.

Table 4 Average major element and REE concentrations in arfvedsonite, early aegirine (Aeg(E)), late aegirine (Aeg(L)) and aegirine containing finely disseminated hematite (Aeg(H)).

wt.%	Arf	Std (6)	Aeg(E)	Std (10)	Aeg(H)	Std (14)	Aeg(L)	Std (4)
SiO_2	51.4	0.1	53.5	0.08	51.4	0.3	53.5	1.0
TiO_2	0.7	0.1	1.0	0.3	0.9	0.2	1.5	1.3
Al_2O_3	0.2	0.01	0.2	0.07	0.2	0.02	0.2	0.04
FeO	31	0.3	29	0.2	30	0.5	29	1.2
MnO	1.2	0.1	0.3	0.08	1.2	0.2	0.5	0.06
MgO	0.05	0.10	bdl	0.002	0.02	0.02	0.03	0.02
CaO	0.3	0.2	0.1	0.07	0.9	0.5	0.2	0.05
Na_2O	9.9	0.7	14	0.05	13	0.5	13	1.7
K_2O	1.9	0.5	0.003	0.002	0.07	0.2	0.3	0.6
F	1.6	0.3	0.01	0.02	0.07	0.2	0.07	0.1
ZnO	0.9	0.3	0.1	0.08	0.7	0.1	0.3	0.06
ZrO_2	0.2	0.08	0.1	0.06	0.2	0.05	0.1	0.01
Total	98.3		98.7		99.3		98.6	
ppm								
Sc	12	0.4	12	0.7	12	0.8	13	1.8
Y	42	15	13	8.4	55	10	83	35
La	4.3	1.8	2.8	1.7	6.1	5.0	1.1	0.3
Ce	13	5.1	8.2	4.7	13	5.5	3.9	1.1
Pr	1.4	0.4	1.5	0.9	1.3	0.4	0.7	0.2
Nd	7.7	2.6	8.0	4.7	7.2	2.4	4.0	0.7
Sm	1.6	0.6	2.4	1.6	1.4	0.4	4.4	0.6
Eu	0.09	0.05	0.1	0.09	0.08	0.02	0.6	0.2
Gd	1.6	0.9	1.5	1.0	1.2	0.5	8.5	3.4
Tb	0.5	0.2	0.3	0.2	0.4	0.08	2.0	0.8
Dy	5.2	2.4	1.8	1.3	5.4	0.7	15	5.0
Ho	2.1	0.9	0.6	0.4	2.7	0.5	3.2	1.0
Er	12	5.8	4.5	2.9	18	3.6	9.5	3.2
Tm	3.8	1.9	2.0	1.4	6.1	1.5	1.6	0.6
Yb	44	23	32	26	72	19	14	7.4
Lu	9.5	5.2	8.4	7.0	16	4.8	2.7	1.8

[1] - Std – standard deviation

Vasyukova, O. V. and A. E. Williams-Jones. "Direct Measurement of Metal Concentrations in Fluid Inclusions, a Tale of Hydrothermal Alteration and Ree Ore Formation from Strange Lake, Canada." Chemical Geology 483 (Apr 20 2018): 385-96. http://dx.doi.org/10.1016/j.chemgeo.2018.03.003.

Table 5 Sources of data for thermodynamic modelling

Mineral/aqueous complex	Reference
Arf	Calculated using the methods of the (Chermak and Rimstidt, 1989), (Berman and Brown, 1985) and (Holland, 1989) with molar volume of arfvedsonite from Hawthorne (1976).
Aeg	Holland and Powell, 1998
Qtz	Holland and Powell, 1998
Ab	Holland and Powell, 1998
Mc	Holland and Powell, 1998
Nahcolite	Vanderzee, 1982, Robie and Hemingway, 1995
CO_2	Holland and Powell, 1998
$REEF^{++}$	Migdisov et al., 2016
$REECl^{++}$	Migdisov et al., 2016
$REECl_2^{+}$	Migdisov et al., 2016
REE^{+++}	Shock and Helgeson, 1988, Shock et al., 1997
REE^{++}	Shock and Helgeson, 1988, Shock et al., 1997
REE^{+}	Shock and Helgeson, 1988, Shock et al., 1997
$NdOH^{++}$	Wood et al., 2002
$Nd(OH)^{++}$	Wood et al., 2002
$Nd(OH)_3^{0}$	Wood et al., 2002
$REECO_3^{+}$	Haas et al., 1995
$REEHCO_3^{++}$	Haas et al., 1995
$REEOH^{++}$	Haas et al., 1995
$REEO^{+}$	Haas et al., 1995
REEOOH	Haas et al., 1995
$REEO^{--}$	Haas et al., 1995

Vasyukova, O. V. and A. E. Williams-Jones. "Direct Measurement of Metal Concentrations in Fluid Inclusions, a Tale of Hydrothermal Alteration and Ree Ore Formation from Strange Lake, Canada." Chemical Geology 483 (Apr 20 2018): 385-96. http://dx.doi.org/10.1016/j.chemgeo.2018.03.003.

Table 6 Calculated pH of the fluid for different stages in its evolution.

Fluid stage	T°C	Fluid composition, wt.% NaCl eq.	Minerals in equilibrium	pH
2a	425	23	Arfvedsonite, microcline, albite, quartz	10.1
2b	360	14	Arfvedsonite, aegirine, microcline, albite, quartz	9.7
3	300	4	Nahcolite	7.5-9.5
3	300	4	CO_2 (nahcolite crystallises on freezing)	4.9-7.5
3	300	4	CO_2 (no nahcolite on freezing)	≤4.9
3	250	4	CO_2, quartz	3.2
4	220	4	CO_2, quartz	3.1
5	150	19	Hematite	5.3
5	150	19	Aegirine	6.2

Vasyukova, O. V. and A. E. Williams-Jones. "Direct Measurement of Metal Concentrations in Fluid Inclusions, a Tale of Hydrothermal Alteration and Ree Ore Formation from Strange Lake, Canada." Chemical Geology 483 (Apr 20 2018): 385-96. http://dx.doi.org/10.1016/j.chemgeo.2018.03.003.

Table 7 Calculated concentrations of selected REE in the fluid during Stages 4 and 5

Fluid stage	Minerals in equilibrium	T°C	pH	ppm			
				Ce	Nd	Dy	Yb
Stage 5	Aegirine	150	6.2	0.08	0.07	1.9	26.0
Stage 4	Hematite	220	3.0	1.6	1.0	4.3	4.7

Vasyukova, O. V. and A. E. Williams-Jones. "Direct Measurement of Metal Concentrations in Fluid Inclusions, a Tale of Hydrothermal Alteration and Ree Ore Formation from Strange Lake, Canada." Chemical Geology 483 (Apr 20 2018): 385-96. http://dx.doi.org/10.1016/j.chemgeo.2018.03.003.